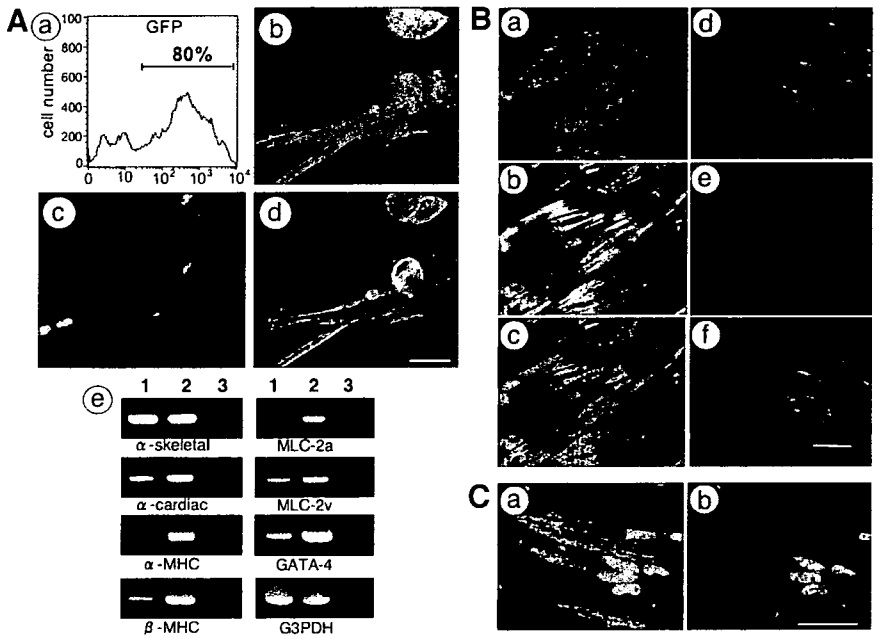

Figure 5. Bone marrow mononuclear cells (BMMNCs) cocultured with brown adipose tissue-derived cells (BATDCs) can contribute to cardiac regeneration. **(A):** Phenotype analysis of cardiomyocytes (CMs) derived from BMMNCs. a, After BMMNCs from green rats were cocultured for 5 days with BATDCs from wild-type rats, FACS analysis showed that 80% of cells were GFP-positive. b–d, Isolated GFP-positive fraction as indicated in panel a were cultured again in the absence of BATDCs for 14 days. Among adherent GFP-positive cells (green) (b), approximately 9.7% showed SA staining (red). d, MEF2C staining (blue) merged with that shown in b and c. e, Reverse transcription-polymerase chain reaction analysis of several CM-specific genes in CMs produced from BMMNCs. Lane 1, cells harvested from the conditions described in b–d (educated BMCs [e-BMCs]); lane 2, CMs from neonatal mice as a positive control; lane 3, total RNA used in lane 1 without reverse transcription. Scale bar = 5 μm. **(B):** Cells obtained as described in **(A)** were injected into infarcted heart, and the tissue distribution of various marker molecules was determined. a–c, GFP (green) (a), SA (blue) (b), and connexin43 (red) merged with that shown in a and b (c). d–f, GFP (green) (d), ANF (red) (e), and nuclear staining with TOPRO3 (blue) merged with that shown in d and e (f). Scale bar = 5 μm (f). **(C):** Fluorescence in situ hybridization staining in implanted site of CM. a, Section was stained with anti-SA (green) and TOPRO3 (blue). b, Serial section of panel a. Green indicates X chromosome, and red indicates Y chromosome. Nuclear staining was performed with TOPRO3 (blue). Cells expressing X and Y chromosome in the nuclei indicate that these cells were derived from e-BMCs and did not fuse with host CM expressing only X chromosome. Scale bar = 5 μm. Abbreviations: G3PDH, glyceraldehyde-3-phosphate dehydrogenase; GFP, green fluorescent protein.

Table 1. Effect of transplanted cells on myocardial performance

	Sham-operated	e-BMCs	Non-e-BMCs	Saline
Echocardiography				
Chamber diameter (mm)	6.11 ± 0.30	7.39 ± 0.70[a,b]	8.09 ± 0.77	10.8 ± 0.58
Viable WT (mm)	1.81 ± 0.17	1.71 ± 0.21[b]	1.70 ± 0.22	1.66 ± 0.13
Infarcted WT (mm)	1.80 ± 0.16	1.35 ± 0.24[a,b]	1.01 ± 0.32	0.75 ± 0.20
% Fractional shortening (%)	78.9 ± 2.1	41.9 ± 3.7[a,b]	33.1 ± 4.3	21.6 ± 2.6

The echocardiography revealed that the experimental infarct group injected with bone marrow mononuclear cells (BMMNCs) cocultured with brown adipose tissue-derived cells (BATDCs) (BMMNCs exposed to BATDCs; e-BMCs) had improved fractional shortening and reduced left ventricular internal dimension at end-diastole compared with the naïve BMMNCs (non-e-BMC)-injected group or the saline-injected group.
[a]Statistically significant difference from bone marrow ($p < .02$).
[b]Statistically significant difference from saline ($p < .01$).
Abbreviations: e-BMC, educated bone marrow cell; WT, wall thickness.

former source of CMs was generated by fusion with donor $CD45^+$ cells, suggesting that plasticity of HSC might result from the fusion of HSCs with resident cells [9]. To reveal which stem cells were capable of differentiating into CMs, we compared an HSC population and a nonhematopoietic MSC population for their ability to differentiate into CMs when cocultured with BATDCs. We sorted $Lin^-c\text{-}Kit^+$ cells and $CD45^-CD31^-CD105^+$ cells in BM from green mice, as typical of HSC and nonhematopoietic MSC populations, respectively (Fig. 6A), and then cocultured them with CD133-positive BATDCs, as shown in Figure 2B. After 14 days, cultured cells were stained with cardiac-specific antigen, which revealed that $SA^+/GATA\text{-}4^+$ cells were generated from both populations; however, the efficiency for differentiation into CMs from those two populations was quite different. As shown in Figure 6B, the number of $SA^+/GATA\text{-}4^+$ CMs from $CD45^-CD31^-CD105^+$ was over 20 times greater than that from $Lin^-c\text{-}Kit^+$ cells (Fig. 6B). These results suggested that nonhematopoietic MSCs are the major source of CMs in the BM.

DISCUSSION

Previously, we showed that BATDCs possessed cardiac progenitor cells, which contributed to the in vivo regeneration of damaged cardiac tissues [9]. Therefore, we suggested that BATDCs might be one of the prospective sources that could overcome issues associated with the regeneration of CMs. In this

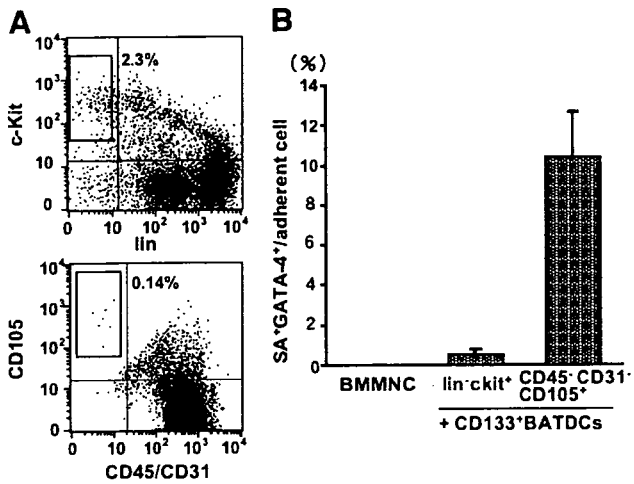

Figure 6. Nonhematopoietic MSCs in bone marrow (BM) mainly differentiate into cardiomyocytes (CMs). **(A):** Cells derived from BM were stained with anti-lineage (mixture of ter119, Mac-1, Gr-1, CD4, CD8, and B220 antibodies) marker or anti-CD31 and anti-CD45 antibodies (*x*-axis) and anti-c-Kit or anti-CD105 antibody (*y*-axis). The percentage of $lin^-c\text{-}Kit^+$ cells and $CD45^-CD31^-CD105^+$ cells in BM are indicated in the box. **(B):** Quantitative evaluation of differentiated SA- and GATA-4-positive CMs from fractionated BMMNCs, as indicated under coculturing with $CD133^+$ BATDCs. Among the adhering BM cells, 10.7% (850 ± 172) and 0.4% (23 ± 3) were $SA^+/GATA\text{-}4^+$ cells from $lin^-c\text{-}Kit^+$ and $CD45^-CD31^-CD105^+$ cells, respectively. BMMNCs alone did not produce CMs. Results represent the mean of five independent experiments. Abbreviations: BATDC, brown adipose tissue-derived cell; BMMNC, bone marrow mononuclear cell.

study, we looked for stem cell markers of CMs in BAT. To this purpose, we compared the capacity for differentiation into CMs from fractionated cells based on the expression levels of c-Kit, Sca-1, and CD133. We could not induce CMs from c-Kit-positive cells, and Sca-1 did not notably increase the numbers of cells that differentiated into CMs. However, there was a remarkable difference in favor of CD133-positive over CD133-negative cells in the ability to differentiate into CMs. Previous studies indicated that CD133 is a common stem cell marker, associated with, for example, neural stem cells, HSCs, endothelial progenitor cells (EPCs), epithelial stem cells, and cancer stem cells. Moreover, it was reported that EPCs differentiated into CMs upon coculturing with neonatal CMs [31]. The results from these previous studies, taken alongside those from our present study, strongly suggest that CD133 might be the CSC marker for stem cell sources in adipose and other tissues. CD133-expressing cells in BAT from the interscapular region were relatively abundant in the embryonic and neonatal stage but were reduced in the adult stage (3.5% vs. 0.2%; data not shown). Moreover, BAT does not exist in great abundance in the adult human. Therefore, BAT itself might not have a clinical application for myocardial disease in adult patients. However, using the evidence that BATDCs can differentiate into CMs and CD133-positive cells from BAT can induce BMMNCs into CMs, we might be able to investigate how BMCs can differentiate into CMs at a molecular level.

In this study, we found that when cocultured in vitro with BATDC, BMCs themselves can give rise to CMs effectively without cell fusion. In the coculture system on $CD133^+$ BATDCs, 1×10^5 total BMMNCs, which logically contained about 140 $CD45^-CD31^-CD105^+$ cells, generated 520 SA^+GATA4^+ cells. On the other hand, in the coculture of nonhematopoietic cells from BM with $CD133^+$ BATDCs, 1×10^4 $CD45^-CD31^-CD105^+$ cells generated approximately 850 SA^+GATA4^+ cells. This low efficiency of induction for CMs from $CD45^-CD31^-CD105^+$ cells may have been due to the lack of other adherent cells observed in the culture using total BMMNCs. At present, we could not determine which adherent cells from BMMNCs were important; however, macrophage and/or endothelial cells may play a role in the generation of CMs synergistically with $CD133^+$ BATDCs.

In the coculture system, when cell-to-cell contact coculture conditions were compared with this filter-separated coculture system, the former effectively induced BMCs into CMs. The culture supernatant of cultured BATDCs, even concentrated, induced BMCs into CMs with an efficiency similar to that observed in the separate coculture conditions. These results suggested that there might be two independent ways of inducing CMs from BMCs. One way is to use the fact that secreted factors determine the fate of BMCs into CMs and the other is that membrane proteins do. With respect to the latter, we suggested that cadherins may mediate this crucial cell-to-cell contact. For the physical interaction of cohering cells, cadherins regulate diverse signaling process, such as differentiation, proliferation, and migration. As previously reported, Ecad-mediated cell-cell interaction, among cells that contain primordial germ cell precursors, is essential to directing such cells to the germ cell fate [30]. In the case of CM development, there is no report showing cadherin-dependent cell commitment; however, an important role for the wnt-frizzled pathway, which is closely related to cadherin, in cardiac development was reported previously [32]. Indeed, calcium depletion with EDTA or EGTA, which prevents cadherin-mediated cell-to-cell contact, abolished the adhesion of BMMNCs to CMs. In addition, cadherins are expressed in GFP^+ BMMNC-derived cells and are localized to the sites of cell-to-cell contact between BMMNCs and BAT CMs (Fig. 4A). Among several type of cadherins, we detected that the suppression of Ecad function was effective in inhibiting both the adhesion of BMMNCs to BATDCs and their differentiation into CMs (Fig. 4B). These data suggest a potential role of Ecad in the differentiation of BMMNCs into CMs. However, additional experiments will be necessary to show the molecular mechanisms behind the cell fate decision that involve cell-to-cell contact. Moreover, regarding the possibility of the existence of a secreted factor from BATDCs for the induction of BMCs into CMs, we found that $CD133^+$ cells expressed platelet-derived growth factor (PDGF)-AB (data not shown), and BMCs expressed platelet-derived growth factor receptor α (PDGFR-α) (data not shown). To understand the contribution of the PDGF-PDGFR system, we added neutralizing antibody against PDGFR-α into the coculture of $CD133^+$ BATDCs and BMCs. Some inhibition of the differentiation from BMCs into SA^+GATA4^+ CMs was observed after 14 days of culturing (data not shown). Moreover, we found that BATDCs expressed beneficial cytokines, such as vascular endothelial growth factor (VEGF), hepatocyte growth factor (HGF), and angiopoietin-1 (data not shown). These and other, unknown factors induced the proliferation and antiapoptotic effect of e-BMCs and contributed to the effective differentiation into SA^+GATA4^+ CMs. With these data, taken together, we confirmed that there might be two processes involved in the effective induction of BMCs into CMs: a secreted protein and cell-to-cell contact mediated by a membrane-binding protein.

With the in vivo infarction model, e-BMCs effectively differentiated into CMs and improved cardiac function. In regard to this point, we found that VEGF and HGF were highly expressed by e-BMCs compared with non-e-BMCs. Moreover, approximately twice the number of $CD31^+$ ECs was observed in the transplanted region of e-BMCs compared with that of non-e-BMCs, and we also found that a small number of e-BMCs incorporated as $CD31^+$ ECs or α-smooth muscle $actin^+$ mural cells (data not shown). These results indicated that the paracrine

effect on neighboring cardiac myocytes and angiogenesis also contributed to the beneficial effects of transplantation.

Furthermore, we found no significant difference in the total number of GFP-positive cells located around the ischemic border zone between BMMNCs exposed to BATDCs (educated BMMNCs) and noneducated BMMNCs; however, SA^+/GFP^+ CMs derived from educated BMMNCs were more than 15 times more abundant in number compared with those from noneducated BMMNCs. Recently, some groups have indicated that VEGFR-2^+/VE-$cadherin^-$ primitive cells from embryonic stem cells do not contribute to vascular cells, such as ECs or SMCs. By contrast, differentiated VE-$cadherin^+$ EPCs contributed to the vascular formation as ECs [33]. These studies suggested that committed immature cells are better sources for vascular or myocardial regeneration than undirected mesodermal-derived stem cells.

In summary, we suggest that CD133-positive cells in BATDCs form an enriched stem cell population, as well as being effective inducers from MSCs in BM to CMs in vitro and in vivo. CD133-positive cells in BATDCs might prove to have potential for the regeneration of CMs.

ACKNOWLEDGMENTS

We thank Dr. M. Okabe (Osaka University, Osaka, Japan) for providing green mice and green rats and M. Sato for technical support. This study was supported in part by a grant from the Ministry of Education, Culture, Sports, Science and Technology of Japan (N.T.).

DISCLOSURE OF POTENTIAL CONFLICTS OF INTEREST

The authors indicate no potential conflicts of interest.

REFERENCES

1 Orlic D, Kajstura J, Chimenti S et al. Bone marrow cells regenerate infarcted myocardium. Nature 2001;410:701–705.
2 Jackson KA, Majka SM, Wang H et al. Regeneration of ischemic cardiac muscle and vascular endothelium by adult stem cells. J Clin Invest 2001;107:1395–1402.
3 Toma C, Pittenger MF, Cahill KS et al. Human mesenchymal stem cells differentiate to a cardiomyocyte phenotype in adult murine heart. Circulation 2002;105:93–98.
4 Makino S, Fukuda K, Miyoshi S et al. Cardiomyocytes can be generated from marrow stromal cells in vitro. J Clin Invest 1999;103:697–705.
5 Tomita S, Li RK, Weise RD et al. Autologous transplantation of bone marrow cells improves damaged heart function. Circulation 1999;100: 247–256.
6 Murry CE, Soonpaa MH, Reinecke H et al. Haematopoietic stem cells do not transdifferentiate into cardiac myocytes in myocardial infarcts. Nature 2004;428:664–668.
7 Balsam LB, Wagers AJ, Christensen JL et al. Haematopoietic stem cells adopt mature haematopoietic fates in ischaemic myocardium. Nature 2004;428:668–673.
8 Alvarez-Dolado M, Pardal R, Garcia-Verdugo JM et al. Fusion of bone-marrow-derived cells with Purkinje neurons, cardiomyocytes and hepatocytes. Nature 2003;425:968–973.
9 Yamada Y, Wang X-D, Yokoyama S-I et al. Cardiac progenitor cells in brown adipose tissue repaired damaged myocardium. Biochem Biophys Res Commun 2006;342:662–670.
10 Weigmann A, Corbeil D, Hellwing A et al. Prominin, a novel microvilli-specific polytopic membrane protein of the apical surface of epithelial cells, is targeted to plasmalemmal protrusions of non-epithelial cells. Proc Natl Acad Sci U S A 1997;94:12425–12430.
11 Yin AH, Miraglia S, Zanjani E et al. AC133, a novel marker for human hematopoietic stem and progenitor cells. Blood 1997;90:5002–5012.
12 Peichev M, Naiyer AJ, Pereira D et al. Expression of VEGFR-2 and AC133 by circulating human CD34(+) cells identifies a population of functional endothelial precursors. Blood 2000;95:952–958.
13 Uchida N, Buck DW, He D et al. Direct isolation of human central nervous system stem cells. Proc Natl Acad Sci U S A 2000;97: 14720–14725.
14 Corbeil D, Roper K, Hellwig A et al. The human AC133 hematopoietic stem cell antigen is also expressed in epithelial cells and targeted to plasm membrane protrusions. J Biol Chem 2000;275:5512–5520.
15 Richardson GD, Robson CN, Lang SH et al. CD133, a novel marker for human prostatic epithelial stem cells. J Cell Sci 2004;117:3539–3545.
16 Torrente Y, Belicchi M, Sampaolesi M et al. Human circulating AC133+ stem cells restore dystrophin expression and ameliorate function in dystrophic skeletal muscle. J Clin Invest 2004;114:182–195.
17 Maw MA, Corbeil D, Koch J et al. A frameshift mutation in prominin-(mouse)-like 1 causes human retinal degeneration. Hum Mol Gen 2000; 9:27–34.
18 Singh SK, Hawkins C, Clarke ID et al. Identification of human brain tumour initiating cells. Nature 2004;432:396–401.
19 Yamada Y, Takakura N. Physiological pathway of differentiation of hematopoietic stem cell population into mural cells. J Exp Med 2006; 203:1055–1065.
20 Yamada Y, Takakura N, Yasue H et al. Exogenous clustered neuropilin 1 enhances vasculogenesis and angiogenesis. Blood 2001;97:1671–1678.
21 Oh H, Bradfute SB, Gallardo TD et al. Cardiac progenitor cells from adult myocardium: Homing, differentiation, and fusion after infarction. Proc Natl Acad Sci U S A 2003;100:12313–12318.
22 Moretti A, Caron L, Nakano A et al. Multipotent embryonic isl1+ progenitor cells lead to cardiac, smooth muscle, and endothelial cell diversification. Cell 2006;127:1151–1165.
23 Wu SM, Fujiwara Y, Cibulsky SM. Developmental origin of a bipotential myocardial and smooth muscle cell precursor in the mammalian heart. Cell 2006;127:1137–1150.
24 Ito T, Suzuki A, Okabe M et al. Application of bone marrow-derived stem cells in experimental nephrology. Exp Nephrol 2001;9:444–450.
25 Zuk PA, Zhu M, Ashjian P et al. Human adipose tissue is a source of multipotent stem cells. Mol Biol Cell 2002;13:4279–4295.
26 Planat-Bénard P, Menard C, Andre M et al. Spontaneous cardiomyocyte differentiation from adipose tissue stroma cells. Circ Res 2004;94: 223–229.
27 Beltrami AP, Barlucchi L, Torella D et al. Adult cardiac stem cells are multipotent and support myocardial regeneration. Cell 2003;114: 763–776.
28 Okabe M, Ikawa M, Kominami K et al. 'Green mice' as a source of ubiquitous green cells. FEBS Lett 1997;407:313–319.
29 Terada N, Hamazaki T, Oka M et al. Bone marrow cells adopt the phenotype of other cells by spontaneous cell fusion. Nature 2002;416: 542–545.
30 Okamura D, Kimura T, Nakano T et al. Cadherin-mediated cell interaction regulates germ cell determination in mice. Development 2003;130: 6423–6430.
31 Badorff C, Brandes RP, Popp R et al. Transdifferentiation of blood-derived human adult endothelial progenitor cells into functionally active cardiomyocytes. Circulation 2003;107:1024–1032.
32 Nakamura T, Sano M, Songyang Z et al. A Wnt-and beta-catenin-dependent pathway for mammalian cardiac myogenesis. Proc Natl Acad Sci U S A 2003;100:5834–5829.
33 Sone M, Itoh H, Yamashita J et al. Different differentiation kinetics of vascular progenitor cells in primate and mouse embryonic stem cell. Circulation 2003;107:2085–2088.


See www.StemCells.com for supplemental material available online.

Neuroscience 144 (2007) 1425–1435

EXPRESSION OF ANGIOGENIC AND NEUROTROPHIC FACTORS IN THE PROGENITOR CELL NICHE OF ADULT MONKEY SUBVENTRICULAR ZONE

A. B. TONCHEV,[a,b] T. YAMASHIMA,[a*] J. GUO,[a]
G. N. CHALDAKOV[b] AND N. TAKAKURA[c1]

[a]*Department of Restorative Neurosurgery, Division of Neuroscience, Kanazawa University Graduate School of Medical Science, Takaramachi 13-1, Kanazawa, 920-8641 Japan*

[b]*Division of Cell Biology, Department of Forensic Medicine, Medical University of Varna, Varna, Bulgaria*

[c]*Department of Stem Cell Biology, Cancer Research Institute, Kanazawa University, Kanazawa, Japan*

Abstract—The subventricular zone along the anterior horn (SVZa) of the cerebral lateral ventricle of adult mammals contains multipotent progenitor cells, which supposedly exist in an angiogenic niche. Numerous signals are known to modulate the precursor cell proliferation, migration or differentiation, in rodent models. In contrast, the data on signals regulating the primate SVZa precursors *in vivo* are scarce. We analyzed the expression at protein level of a panel of angiogenic and/or neurotrophic factors and their receptors in SVZa of adult macaque monkeys, under normal condition or after transient global ischemia which enhances endogenous progenitor cell proliferation. We found that fms-like tyrosine kinase 1 (Flt1), a receptor for vascular endothelial cell growth factor, was expressed by over 30% of the proliferating progenitors, and the number of Flt1-positive precursors was significantly increased by the ischemic insult. Smaller fractions of mitotic progenitors were positive for the neurotrophin receptor tropomyosin-related kinase (Trk) B or the hematopoietic receptor Kit, while immature neurons expressed Flt1 and the neurotrophin receptor TrkA. Further, SVZa astroglia, ependymal cells and blood vessels were positive for distinctive sets of ligands/receptors, which we characterized. The presented data provide a molecular phenotypic analysis of cell types comprising adult monkey SVZa, and suggest that a complex network of angiogenic/neurotrophic signals operating in an autocrine or paracrine manner may regulate SVZa neurogenesis in the adult primate brain.

Key words: cerebral ischemia, primate, neurogenesis, Flt1, TrkB, Kit.

The subventricular zone of the anterior horn (SVZa) of the cerebral lateral ventricle in adult mammals harbors neural progenitor cells which are capable of glial and neuronal production. These cells have been studied extensively in non-primate mammalian species, and a number of molecular signals that affect their proliferation and differentiation have been identified (reviewed by Okano, 2002; Lledo et al., 2006). Cerebral injuries such as ischemia up-regulate SVZa progenitors in both focal (Jin et al., 2001; Zhang et al., 2001; Arvidsson et al., 2002; Parent et al., 2002) and global (Iwai et al., 2003) rodent ischemic models. The ischemia-triggered activation of endogenous precursors can be further enhanced by external application of trophic factors (reviewed by Zhang et al., 2005; Lichtenwalner and Parent, 2006). Existence of progenitor cells was described also in SVZa of normal adult primates, including both humans (Pincus et al., 1998; Sanai et al., 2004) and monkeys (Kornack and Rakic, 2001; Pencea et al., 2001a). Recently, we reported evidence that, similarly to the rodent brain, ischemia was capable of increasing the proliferation of SVZa precursors in a monkey model of transient global cerebral ischemia (Tonchev et al., 2005). Whether these similar responses between rodents and monkeys are mediated by identical or distinct molecular signals is currently unknown as the knowledge on the molecular regulation of primate SVZa progenitors is limited.

Recent evidence indicates that neural and vascular cells not only reciprocally affect their own growth by paracrine mechanisms (reviewed by Emanueli et al., 2003), but also use common signals (reviewed by Carmeliet, 2003). For example, neurotrophins such as nerve growth factor (NGF) and brain-derived neurotrophic factor (BDNF) promote angiogenesis (Calza et al., 2001; Kim et al., 2004). Reciprocally, vascular signaling affects neuronal precursor cells (Leventhal et al., 1999; Palmer et al., 2000; Palmer, 2002; Yamashima et al., 2004). In addition to its well-known role in angiogenesis, vascular endothelial growth factor (VEGF) promotes neurogenesis and neuroprotection by mediating both proliferation (Jin et al., 2002a) and chemoattraction (Zhang et al., 2003) of adult brain progenitors, under normal or ischemic (Sun et al., 2003) conditions. Importantly, a link between angiogenic and neurotrophic factors in regulating adult neurogenesis was established, by showing that endothelial cell-derived VEGF enhances neurogenesis in a BDNF-dependent manner (Louissaint et al., 2002).

In the present study, we investigated the expression at protein level of angiogenic and/or neurotrophic factors and their receptors in the progenitor cell niche of adult monkey

[1] Present address: Department of Signal Transduction, Research Institute for Microbial Diseases, Osaka University, Osaka, Japan.

*Corresponding author. Tel: +81-76-265-2381; fax: +81-76-231-1718.
E-mail address: yamashim@med.kanazawa-u.ac.jp (T. Yamashima).

Abbreviations: ac, anterior commissure; Ang, angiopoietin; BDNF, brain-derived neurotrophic factor; BrdU, bromodeoxyuridine; Flk, fetal liver kinase; Flt, fms-like tyrosine kinase; GDNF, glial cell line-derived neurotrophic factor; GFRα1, glial cell line-derived neurotrophic factor family receptor α1; NGF, nerve growth factor; Nrp, neuropilin; NT3, neurotrophin-3; PI, propidium iodide; SCF, stem cell factor; SVZa, anterior subventricular zone; Tie, tyrosine kinase with immunoglobulin-like and epidermal growth factor-like domains; TRITC, tetramethylrhodamine isothiocyanate; Trk, tropomyosin-related kinase; VEGF, vascular endothelial growth factor; vWF, von Willebrand factor.

0306-4522/07$30.00+0.00
doi:10.1016/j.neuroscience.2006.10.052

SVZa. We employed a primate model that has previously demonstrated an increased proliferation of SVZa precursors after ischemia (Tonchev et al., 2005). Our target was to determine the receptor(s) expressed by actively proliferating precursors as well as by other cellular phenotypes comprising SVZa, and thus to provide structural evidence for putative ligand/receptor interactions in adult monkey progenitor cell niche. Such evidence may be helpful in designing future studies devoted on establishing the precise involvement of each of the studied factors in the regulation of primate progenitor cells.

EXPERIMENTAL PROCEDURES

Animal procedures

Animal experiments were performed under strict adherence to the guidelines of the Animal Care and Ethics Committee of Kanazawa University, and the NIH Guide for the Care and Use of Laboratory Animals. All efforts were made to minimize the number of animals used and to reduce animal suffering throughout the experiments. The subjects of investigation were adult Japanese monkeys (*Macaca fuscata*), bred in air-conditioned cages, and allowed free daily access to food and water. A model of transient global cerebral ischemia was performed as previously described (Yamashima et al., 1998; Tonchev et al., 2005). Briefly, the sternum was resected under general anesthesia with artificial ventilation, and the innominate and left subclavian arteries were transiently ligated for 20 min. The effectiveness of clipping was demonstrated by an almost complete absence (0.5±1.0 ml/100 g brain/min) of cerebral blood flow as monitored by laser Doppler (Vasamedics, St. Paul, MN, USA). Ischemia was performed on six monkeys, while two monkeys underwent sham surgery (executed by opening the chest without vessel clipping). All monkeys received five daily injections of 100 mg/kg i.v. of bromodeoxyuridine (BrdU) (Sigma-Aldrich Japan K.K., Tokyo, Japan), performed on days 5–9 after surgery. Respective animals were then killed on day 9 (n=2), day 23 (n=2) and day 44 (n=2) and after ischemia or on day 9 (n=2) after the sham operation (Tonchev et al., 2005).

Histological processing

The monkeys were killed by lethal doses of sodium pentobarbital and intracardially perfused with ice-cold saline containing heparin followed by ice-cold solution of 4% paraformaldehyde. Upon removal of brain, tissue blocks corresponding to anterior commissure (ac) +7 mm anteriorly until ac +1 mm posteriorly were resected and submerged in 30% sucrose solution until they sank to the bottom. The tissues were then frozen in O.C.T. medium (Tissue-Tek, Sakura Finetech Co., Tokyo, Japan), and serially cut into 40-μm thick coronal sections. All stainings were performed on free-floating sections. Upon equilibrating sections in Tris-buffered saline containing 0.1% Triton X-100 (TBS-T) and appropriate blocking sera, the primary antibodies were applied (Table 1) for 48 h at 4 °C. We tested whether the use of the detergent Triton X-100 may prevent the successful immunostaining of membranous antigens such as the receptors of signaling molecules targeted in our study; in pilot experiments we used concentrations ranging from 0.01% to 0.1% Triton as well as no Triton in the buffer. As we did not observe differences among these formulations in respect to the quality of staining, we used 0.1% Triton because we thought it would provide a better reagent penetration in the 40-μm thick sections. VEGF was investigated concomitantly with its two principal receptors acting in the nervous system: the receptor tyrosine kinases fms-like tyrosine kinase (Flt) 1 and fetal liver kinase (Flk) 1, and the co-receptor Neuropilin 1 (Nrp1) (Fer-

Table 1. List of primary antibodies against signaling molecules and their receptors used in the study

Antibody against	Epitope	Species	Dilution	Reference	Vendor, cat. #
VEGF	N-terminus of human VEGF-A	Goat	1:200	Ruef et al., 1997	Santa Cruz Biotechnology (Santa Cruz, CA, USA); #sc-152
Flt1	Amino acids 23–247 of human Flt1	Rabbit	1:100	Tissot van Patot et al., 2004	Santa Cruz; #sc-9029
Flk1	Amino acids 1158–1345 of mouse Flk1	Rabbit	1:50	Ruef et al., 1997	Santa Cruz; #sc-504
Nrp1	Amino acids 570–855 of human Nrp1	Rabbit	1:200	Parikh et al., 2004	Santa Cruz; #sc-5541
Kit tyrosine kinase receptor	Amino acids 961–976 of human Kit	Rabbit	1:50	Gougeon and Busso, 2000	Calbiochem (LA Jolla, CA, USA); #PC34
Ang1	N-terminus of human Ang1	Goat	1:50	Otani et al., 1999	Santa Cruz; #sc-6319
Ang2	N-terminus of human Ang2	Goat	1:50	Otani et al., 1999	Santa Cruz; #sc-7016
Tie2	C-terminus of mouse Tie2	Rabbit	1:100	Otani et al., 1999	Santa Cruz; #sc-324
Tie1	C-terminus of human Tie1	Rabbit	1:100	Uchida et al., 2000	Santa Cruz; #sc-342
NGF	Amino acids 1–20 of human NGF	Rabbit	1:200	Quartu et al., 1999	Santa Cruz; #sc-548
BDNF	Amino acids 1–20 of human BDNF	Rabbit	1:200	Hayashi et al., 2001	Santa Cruz; #sc-546
NT3	Amino acids 139–158 of human NT3	Goat	1:200	Quartu et al., 1999	Santa Cruz; #sc-13380
TrkA	Amino acids 763–777 of human TrkA	Rabbit	1:200	Quartu et al., 2003	Santa Cruz; #sc-118
TrkB	Amino acids 794–808 of mouse TrkB	Rabbit	1:200	Hayashi et al., 2000	Santa Cruz; #sc-12
TrkC	Amino acids 798–812 of porcine TrkC	Rabbit	1:200	Sandell et al., 1998	Santa Cruz; #sc-117
Pan-neurotrophin receptor of 75 kD (p75NTR)	Amino acids 1–160 of human p75	Mouse	1:50	Sandell et al., 1998	Dako (Kyoto, Japan); #M3507
GDNF	Recombinant human GDNF	Goat	1:100	Serra et al., 2002	R&D Systems (Minneapolis, MN, USA); #AF-212-NA
GFRα1	Amino acids 368–437 of human GFRα1	Rabbit	1:200	Serra et al., 2005	Santa Cruz; #sc-10716
Ret tyrosine kinase receptor	C-terminus of human Ret	Goat	1:200	Walker et al., 1998	Santa Cruz; #sc-1290

References describe previous use of each antibody in primate neural or non-neural tissues.

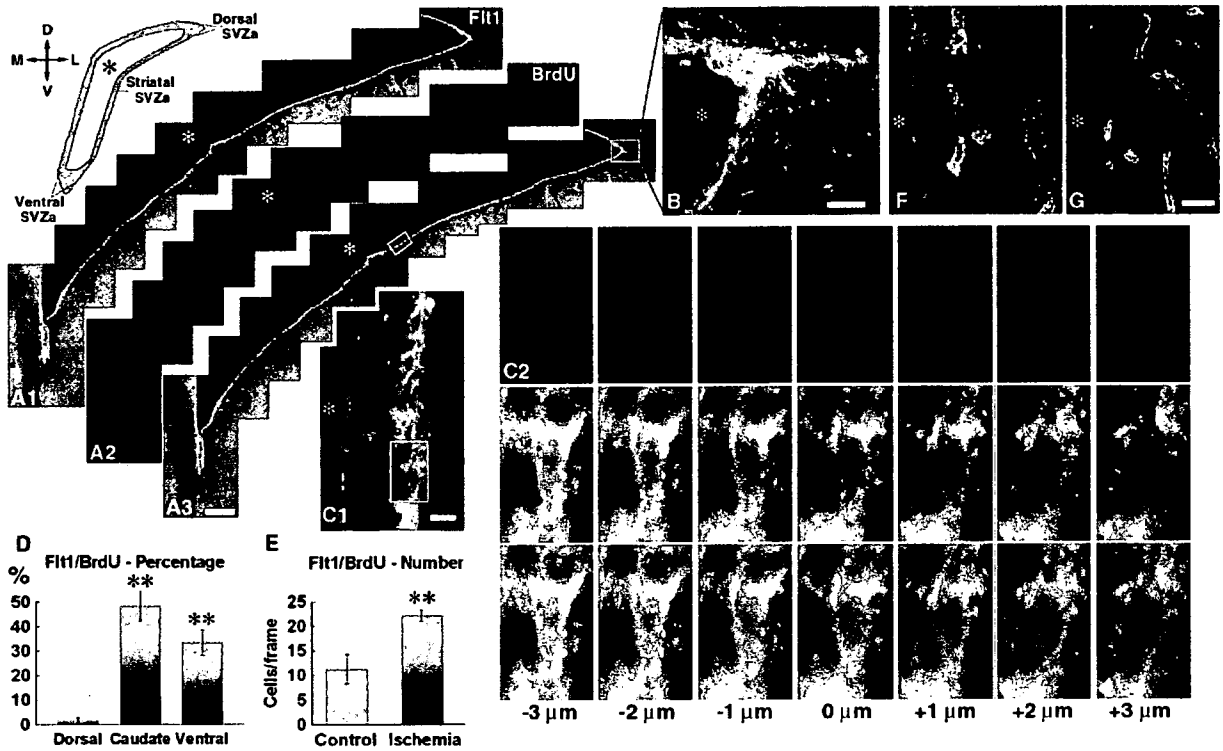

Fig. 1. Expression of Flt1 in SVZa. (A) Photomontages of low magnification micrographs showing the distribution of Flt1 (A1) and BrdU (A2) positive signals in SVZa, and overlay (A3). The positions of the SVZa aspects are depicted on the schematic map (upper left; D, dorsal; V, ventral; M, medial; L, lateral). Note that both $Flt1^+$ and $BrdU^+$ cells are preferentially localized along the lumen of the ventricle. (B) Higher power view of Flt1 (green) and BrdU (red) double-staining on day 9 in dorsal SVZa. Note lack of double-stained cells. (C) Flt1 and BrdU (red) double-staining in striatal SVZa on day 9. (C1) A $Flt1^+/BrdU^+$ cell cluster is focused (frame). (C2) The cluster is presented as consecutive 1-μm optical sections in the *z* axis to demonstrate the co-localization of the signals (the Flt1 signal is shown in white to achieve a better contrast). (F) Percentage of $BrdU^+$ cells co-labeled for Flt1 in various SVZa aspects. * $P<0.01$ versus dorsal SVZa. (G) Absolute number of $BrdU^+$ cells co-labeled for Flt1 in control and postischemic SVZa (dorsal, striatal, ventral). ** $P<0.01$ versus control. Expression of Flk1 in SVZa, and control stainings. The top panel shows Flk1 immunoreactivity in a subependymal blood vessel (bv). Positive cells outside the vascular wall are absent. The bottom panels depict negative control stainings by omitting primary antibody. Similar results were obtained by using pre-adsorption with specific blocking peptides. Scale bars=400 μm (A); 40 μm (B); 10 μm (C); 50 μm (D, E). Asterisk, lateral ventricle.

rara et al., 2003). Kit (CD117), the receptor for stem cell factor (SCF), might be implicated in angiogenesis by its expression on hematopoietic and circulating endothelial progenitor cells (Li et al., 2003). SCF stimulates endogenous neural progenitor cells after cerebral ischemia in rodents (Jin et al., 2002b; Kawada et al., 2006). We investigated NGF, BDNF and their cognate receptors, because both NGF (Calza et al., 2003) and BDNF *in vivo* affect SVZa progenitors in rodents (Pencea et al., 2001b; Benraiss et al., 2001) and monkeys (Bedard et al., 2006). We particularly noticed the relation of neurotrophin and VEGF immunoreactivities (Calza et al., 2001; Louissaint et al., 2002). Other neurotrophic factors, neurotrophin-3 (NT3) (Ghosh and Greenberg, 1995) and glial cell line-derived neurotrophic factor (GDNF) (Chen et al., 2005), have also been reported to affect brain progenitor cells in rodent models, and GDNF was implicated in postischemic precursor proliferation (Dempsey et al., 2003), but their involvement in the primate progenitor cell niche is unclear; thus they were investigated.

In addition to antibodies directed against signaling molecules or their receptors, we used the following antibodies against phenotypic markers: mouse anti-BrdU (1:100, Becton Dickinson, San Jose, CA, USA), rat anti-BrdU (1:100, Harlan Sera-Laboratory, Loughborough, UK), mouse anti-Nestin (Chemicon, Temecula, CA, USA), rabbit or mouse anti-β-tubulin class III (1:400, Covance, Richmond, CA, USA), rabbit anti-glial fibrillary acidic protein (GFAP) (1:400, Sigma; or DAKO Japan K.K., Kyoto, Japan), mouse anti-S100β (1:500, Sigma), mouse anti-CD31 (1:50, DAKO), and rabbit anti-von Willebrand factor (vWF) (1:200; DAKO). To reveal BrdU incorporated into DNA of cells, DNA was denatured by sequentially incubating sections in formamide and HCl as described (Tonchev et al., 2005), followed by application of primary antibodies. The primary antibodies were revealed by appropriate secondary antibodies conjugated to AlexaFluor 488, 546, or 633 (Molecular Probes, Eugene, OR, USA), tetramethylrhodamine isothiocyanate (TRITC; Jackson Immunoresearch, West Grove, PA, USA), or to biotin for immunoperoxidase labeling (1:30–1:100; Vector ABC kit, Vector Laboratories, Burlingame, CA, USA). For double- and triple-staining, primary antibodies were from different species, and were applied sequentially to minimize the probability for cross-reactivity. For Flt1/Kit double-staining using two rabbit antibodies, just before the second primary, the first primary was masked by a large excess of unconjugated secondary antibody (anti-rabbit IgG; Vector) (Lewis Carl et al., 1993; Muzio et al., 2002).

Antibody specificity

All of the antibodies used in the present study have been previously characterized on primate (monkey or human) tissues (see references list in Table 1). The antibodies directed against neu-

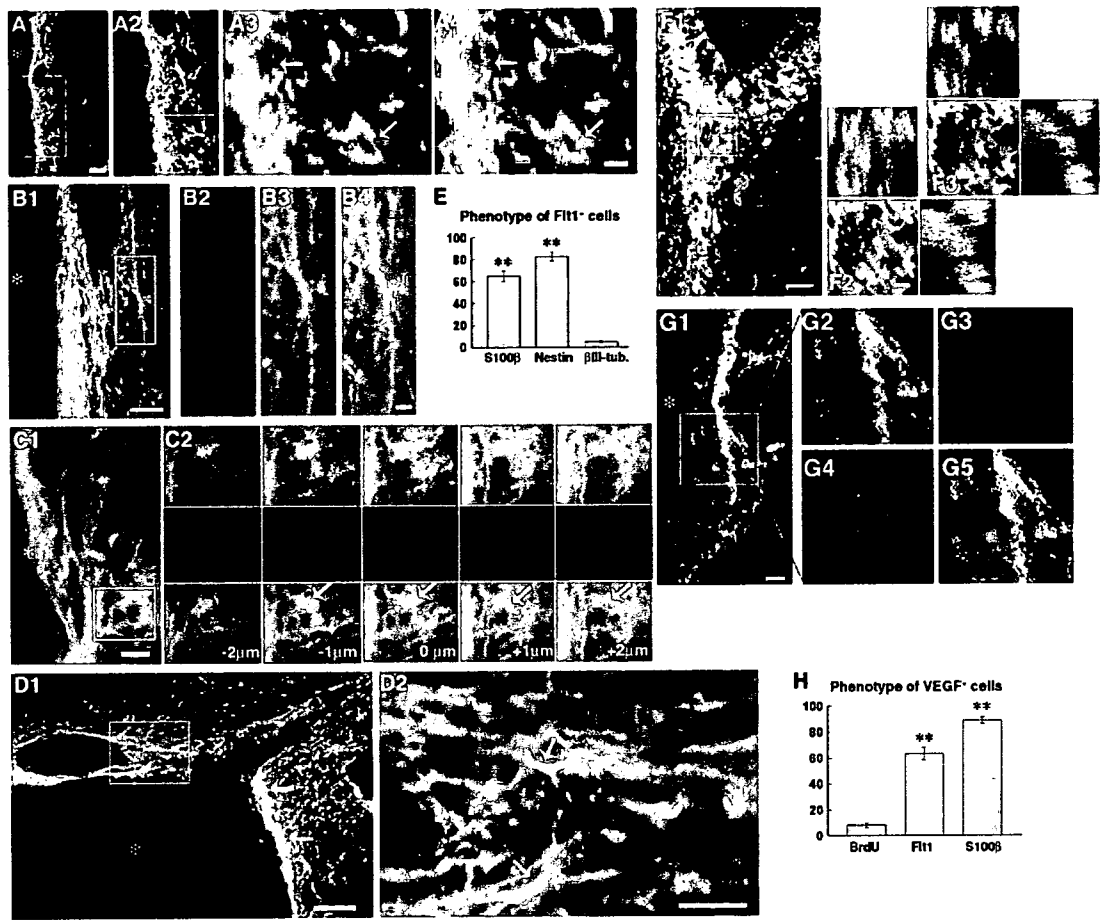

Fig. 2. Phenotype of Flt1$^+$ and VEGF$^+$ cells in SVZa. (A) Double-staining for Flt1 (green) and S100β (red) on day 9. The boxed region in A1 is magnified in A2, and the boxed region on A2 is magnified with channel separation in A3. Flt1$^+$/S100β^+ cells appear yellow (arrows). (B) Double-staining for Flt1 (green) and nestin (red) on day 9. The boxed region in B1 is magnified with channel separation in B2–B4. (C) Double-staining for Flt1 (green) and βIII-tubulin (red) on day 44. The cluster depicted by a box (C1) is shown as consecutive optical sections in the z axis (C2) to confirming the co-localization of the signals (a 3D reconstruction of this cluster is presented in Supplementary movie 2). (D) Double-labeling for Flt1 (green) and VEGF (red) on day 9 in dorsal SVZa. Boxed area in D1 is magnified in D2. Flt1$^+$/VEGF$^+$ cells appear in yellow (the arrow shows an example) while some Flt1$^-$/VEGF$^+$ cells appear in red. (E) Percentages of Flt1$^+$ cells co-labeled for cell markers. ** $P<0.01$ versus βIII-tubulin. (F) Double-staining for VEGF (green) and BrdU (red) on day 23. While many BrdU$^+$ cells are negative for VEGF, a double-labeled cluster (boxed area in F1) is presented with orthogonal projections in the x and y axes in F2 and F3. (G) Triple-labeling for VEGF, S100β and βIII-tubulin on day 9 in striatal SVZa. G1 depicts low magnification overlay view of the three channels, with the boxed area presented with channel separation; G2 (VEGF), G3 (S100β), G4 (βIII-tubulin), G5 (overlay). Note that VEGF$^+$ and βIII-tubulin$^+$ cells are spatially adjacent but distinct. (H) Percentages of VEGF$^+$ cells co-labeled for cell markers. ** $P<0.01$ versus BrdU. Scale bars=50 μm (D1); 20 μm (A1, F1); 10 μm (B1, C1, G1); 5 μm (A4, B4, D2, F2). Asterisk, lateral ventricle.

rotrophins (NGF, BDNF, NT3, GDNF) or their receptors have been characterized on primate brains by both immunohistochemistry and Western blot (Quartu et al., 1999, 2003; Hayashi et al., 2000, 2001; Sandell et al., 1998; Serra et al., 2002, 2005; Walker et al., 1998). Staining monkey brain regions outside of SVZa with these antibodies yielded a pattern similar to the above-cited studies (data not shown). The antibodies directed against angiogenic factors or their receptors have been characterized in non-neural primate tissues (Ruef et al., 1997; Otani et al., 1999; Gougeon and Busso, 2000; Tissot van Patot et al., 2004; Parikh et al., 2004). To determine the specificity of the primary antibodies, these were pre-absorbed with 10-fold excess of blocking peptides, where such peptides were available: anti-VEGF, anti-Nrp1, anti-NGF, anti-BDNF, anti-NT3, anti-tropomyosin-related kinase (Trk) A, anti-TrkB, anti-TrkC, anti-angiopoietin (Ang) 1, anti-Ang2, anti-tyrosine kinase with immunoglobulin-like and epidermal growth factor-like domains (Tie) 1, anti-Tie2, and anti-Ret. Negative control experiments were also performed by omitting the primary antibody. All these control stainings revealed no positivity (Supplementary Fig. 1).

Image analysis

Double- and triple-labeling to determine the expression of signaling molecules or their receptors by BrdU-labeled cells or cells labeled for particular phenotypic markers was evaluated using confocal laser scanning microscopy (LSM 510, Carl Zeiss, Tokyo, Japan). Alexa Fluor 488 was appointed in the green channel, TRITC or Alexa Fluor 546, in the red channel, and Alexa Flour 633, in the blue channel. We undertook specific steps to avoid "leakage" ("bleed-through") of signal among the channels, e.g. to visualize an intense green signal in the red

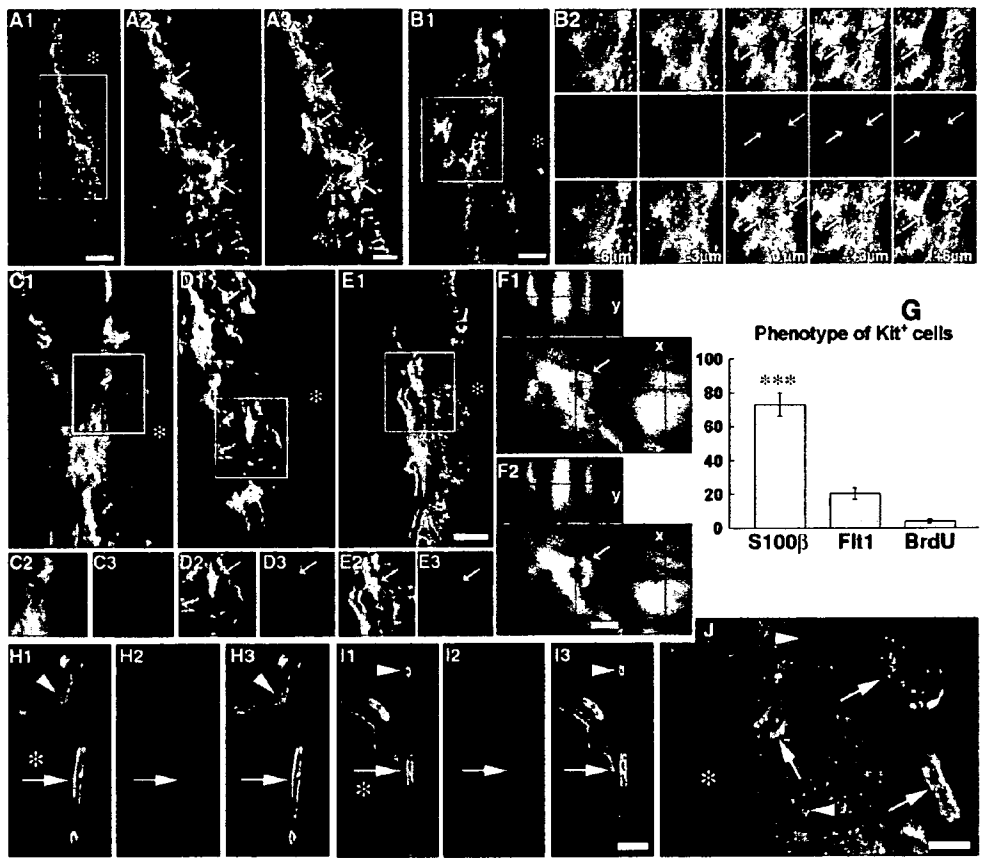

Fig. 3. Phenotype of Kit$^+$ cells in SVZa. (A) Kit immunoreactivity (green) in striatal SVZa, counterstained by PI (red). The boxed region in A1 is magnified with channel separation in A2 and A3. Note the subependymal localization of the Kit$^+$ cells (arrows). (B) Higher magnification view of Kit immunoreactivity (green) in striatal SVZa, counterstained by PI (red). The boxed region in B1 is presented as consecutive 1-μm optical sections in the z axis. Note a PI$^+$ cluster (arrows) does not express Kit, which is confirmed by a 3D reconstruction (Supplementary movie 2). (C) Double-labeling for Kit (green) and βIII-tubulin (red) on day 23. The boxed region in C1 is magnified with channel separation in C2 and C3. (D) Double-labeling for Kit (green) and S100β (red) on day 9. The boxed region in D1 is magnified with channel separation in D2 and D3. A double-positive cell is depicted by arrow. (E) Double-labeling for Kit (green) and Flt1 (red) on day 9. The boxed region in E1 is magnified with channel separation in E2 and E3. A double-positive cell is depicted by arrow. (F) Double-labeling for Kit (green) and BrdU (red) on day 9. A double-positive cell Kit/BrdU cell (arrow) is presented in a merged image (F1) or Kit channel only (F2) with orthogonal projections in the x and y axes. (G) Percentages of Kit$^+$ cells co-labeled for cell markers. *** $P<0.001$ versus Flt1/BrdU. (H) Double-staining for CD31 (H1) and Ang1 (H2), and overlay (H3) in SVZa, day 9. (I) Double-staining for CD31 (I1) and Tie2 (I2), and overlay (I3) in SVZa, day 9. CD31$^+$/Ang1$^+$ and CD31$^+$/Tie2$^+$ vessels are depicted by arrows. Not all blood vessels are positive for Ang1 or Tie2 (CD31$^+$/Ang1$^-$ and CD31$^+$/Tie2$^-$ vessels are depicted by arrowheads). (J) Double-staining for Tie1 (green) and BrdU (red) in SVZa, day 9. Tie1$^+$ blood vessels (arrows) and BrdU$^+$ cells (arrowheads) do not co-label. Asterisk, lateral ventricle. Scale bars=50 μm (A, H, I), 20 μm (B–E, J), 5 μm (F2). Asterisk, lateral ventricle.

channel. Thus, each fluorochrome was assigned to be scanned separately and sequentially to minimize the probability of signal transfer among channels. Z sectioning at 0.5–1 μm intervals was performed and optical stacks of at least 20 images were used for analysis. Digital three-dimensional reconstructions were created by the Zeiss LSM software version 2.3. Within each animal group, at least 150 cells positive for BrdU or a phenotypic marker were sampled for co-expression with respective transcription factors. The absolute numbers of transcription factor/BrdU double-positive cells were determined by multiplying the corresponding fractions with the total numbers of BrdU$^+$ cells evaluated on every 12th section stained by the peroxidase method within grids of 800 μm$\times$100 μm placed in the dorsal, ventral, and striatal aspects of SVZa (see Fig. 1A) as previously described (Tonchev et al., 2005). Numbers and percentages were averaged to obtain a mean density value for each transcription factor/animal group.

Statistical analysis

For comparing percentages of cells expressing certain transcription factor, we applied nonparametric tests (Mann-Whitney U test and Kruskal-Wallis test) or one-way ANOVA followed by Tukey-Kramer's post hoc comparisons. Data were expressed as means±S.E.M. Differences were considered significant when $P<0.05$.

RESULTS

Flt1 was expressed by proliferating progenitors

Staining for Flt1 in monkey SVZa revealed an intense positive signal in the dorsal, striatal and ventral SVZa aspects (Fig. 1A), which showed increased numbers of

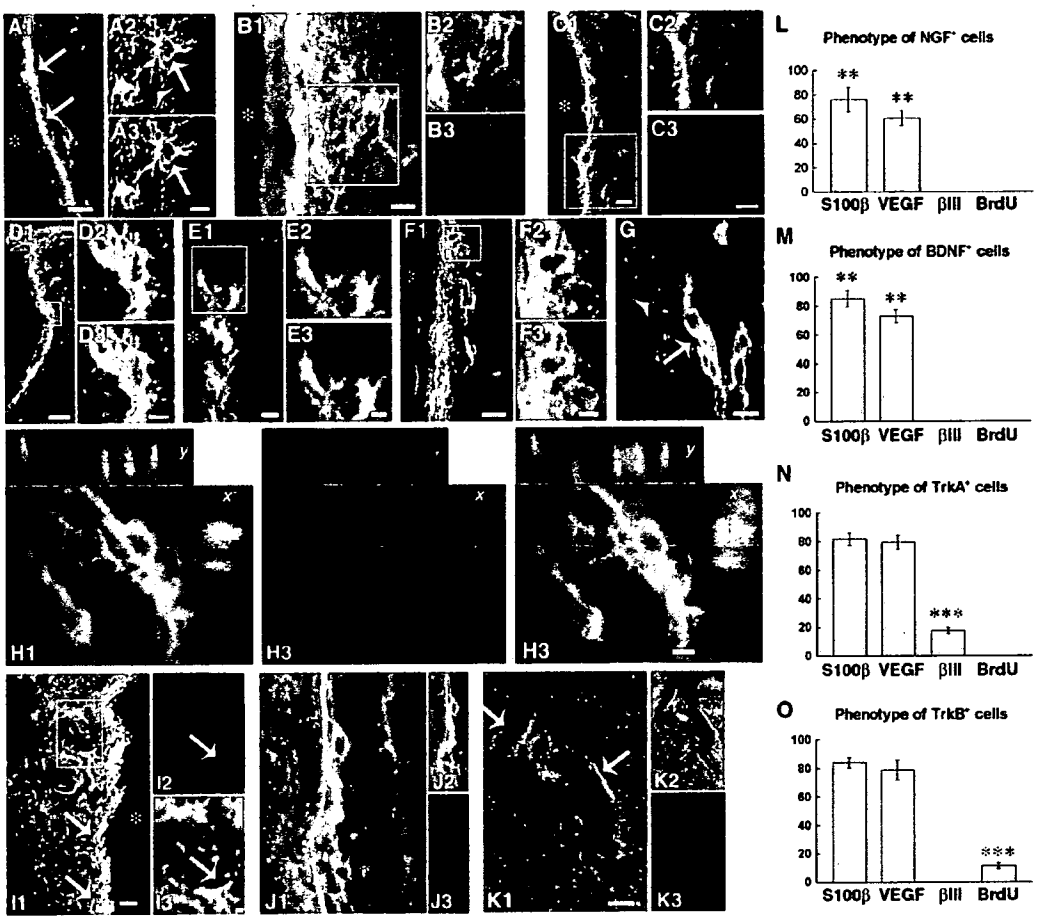

Fig. 4. NGF, BDNF, and their receptors in SVZa. (A) Single-labeling for NGF, day 9 (A1) demonstrating positive band of cells in SVZa (arrows), followed by double-labeling (A2, A3) for NGF (green; arrow) and BrdU (red; arrowhead) demonstrating lack of co-labeling. (B) Double-staining for NGF (green) and S100β (red), control. Double-positive cells appear in yellow. The boxed region in B1 is presented with channel separation in B2 and B3. (C) Double-labeling for NGF (green) and VEGF, day 9. Double-positive cells appear in yellow. The boxed region in C1 is magnified with channel separation in C2 and C3. (D) Double-staining for BDNF (green) and S100β (red), day 9. Double-positive cells appear in yellow. The boxed region in D1 is magnified with channel separation in D2 and D3. (E) Double-labeling for BDNF (green) and βIII-tubulin (red), day 9. The boxed region in E1 is magnified with channel separation in E2 and E3. Note the lack of co-labeling. (F) Double-staining for TrkB (green) and S100β (red), day 9. Double-positive cells appear in yellow. The boxed region in F1 is magnified with channel separation in F2 and F3. (G) Double-staining for TrkA (green; arrows) and BrdU (red; arrowhead), day 9. Note lack of co-labeling. (H) Double-staining for TrkB (H1), BrdU (H2), and overlay (H3), day 9. A double-positive cluster is depicted, with orthogonal projections in the *x* and *y* axes. (I) Double-staining for TrkB (green) and VEGF (red), day 9. Note extensive subependymal co-labeling (arrows). The boxed region in I1 is magnified in I2 and I3 depicting a double-labeled stellate cell (arrows). (J) Double-staining for TrkA (green), and βIII-tubulin (red) in striatal SVZa, day 9. The double-positive cells appear with a honeycomb pattern in yellow. The boxed region in J1 is magnified with channel separation in J2 and J3. (K) Double-staining for 75 kD pan-neurotrophin receptor (p75NTR) and vWF (K1), with channel separations in K2 and K3, day 23. (L–O) Percentages of NGF^+, $BDNF^+$, $TrkA^+$ and $TrkB^+$ cells, respectively, co-labeled for cell markers; ** $P<0.01$; *** $P<0.001$. Scale bars=50 μm (D1); 20 μm (A1, C, F1); 10 μm (A3, B1, D2, E1, G, I1, J, K); 5 μm (E3, F3, H3). Asterisk, lateral ventricle.

proliferating ($BrdU^+$) progenitors after ischemia (Tonchev et al., 2005). Extension of the Flt1 immunoreactivity in the rostral migratory stream toward the olfactory bulb was not observed (Fig. 1A3). Careful investigation for Flt1/BrdU co-labeling under high magnification revealed that in the dorsal SVZa double-stained cells were rare (Fig. 1B), while in the striatal (Fig. 1C) or ventral (Fig. 1D) SVZa such cells were frequently observed. The finding of Flt1/BrdU-labeled clusters (Fig. 1C) was paralleled by data showing formation of $Flt1^+$ clusters in stainings using the DNA-binding dye propidium iodide (PI) to label all nuclei. Significantly higher percentages of $Flt1^+/BrdU^+$ cells were identified in striatal or ventral SVZa as compared with its dorsal aspect (Fig. 1D). Further, ischemia increased the total number of $Flt1^+/BrdU^+$ cells in SVZa on day 9 as compared with controls (Fig. 1E). Flt1/BrdU co-expression at a long-term survival time points (day 23 or 44) was negligible (data not shown). In contrast to Flt1, Flk1 and the VEGF co-receptor Nrp1 were restricted to the vascular wall (Fig. 1F, G), in particular endothelial cells.

Most $Flt1^+$ cells co-labeled with S100β and nestin (Fig. 2A, B, E), with no statistically significant difference between control and ischemic monkeys. Co-staining of Flt1 with the neuronal marker βIII-tubulin was rare (Fig. 2C, E).

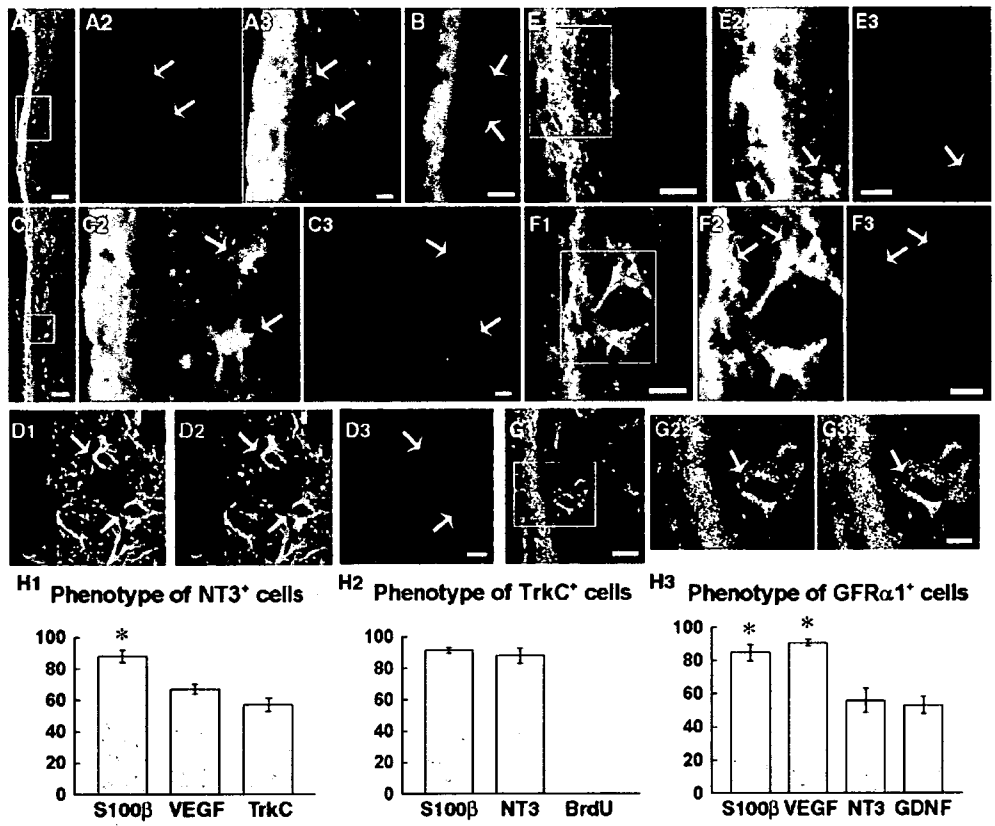

Fig. 5. NT3, GDNF, and their receptors in SVZa. (A) Double-staining for TrkC (green) and NT3 (red), day 9. The boxed zone (A1) is magnified in A2 and A3. In addition to the ependymal layer, some subependymal cells are double-labeled (arrows). (B) Double-staining for TrkC (green) and BrdU (red; arrows), day 9. Note lack of co-labeling. (C) Double-staining for S100β (green) and NT3 (red), day 9. Subependymal astrocytes cells are double-positive (arrows). The boxed region (C1) is magnified in C2 and C3. (D) Double-staining for VEGF (green, D2) and NT3 (red, D3), and overlay (D1), in control SVZa. Double-positive subependymal cell with stellate morphology are depicted by arrows. (E) Triple-labeling for GFRα1 (green), NT3 (red) and S100β (blue), day 9. The boxed region (E1) is magnified with channel separation in E2 and E3. A subependymal GFRα1⁺ cell is co-stained for NT3 (arrow), while the strongly positive for S100β ependyma (appearing in pink in the overlay, A1) is co-labeled for NT3 but not for GFRα1. (F) Triple-labeling for GFRα1 (green), VEGF (red) and S100β (blue), day 9. The boxed region (F1) is magnified with channel separation in F2 and F3. The immunoreactivity of both GFRα1 and VEGF is largely subependymal and co-localizes on perivascular cells (arrows). (G) Double-staining for GFRα1 (green) and GDNF (red), day 9. The boxed zone (G1) is magnified in G2 and G3. A double-stained subependymal blood vessel is depicted by an arrow. (H) Percentages of NT3⁺, TrkC⁺ and GFRα1⁺ cells, respectively, co-labeled for cell markers; * $P<0.05$. Scale bar=50 μm (A1, C1); 20 μm (E1, F1, G1); 10 μm (A3, B, C3, D3, E3, F3, G3). Asterisk, lateral ventricle.

Double-staining for Flt1 and VEGF showed that over half of the VEGF⁺ cells co-expressed Flt1 (Fig. 2D, H). VEGF extensively co-labeled with S100β (Fig. 2G, H) but not with βIII-tubulin (Fig. 2G). Some BrdU⁺ cells, mainly in ventral SVZa, were double-labeled for VEGF (Fig. 2F, H), and VEGF immunoreactivity was also found in the rostral migratory stream, on astrocytes (data not shown). The percentage of VEGF/BrdU co-labeling was significantly lower that the percentage of Flt1/BrdU co-labeling (Kruskal-Wallis Test, $P=0.006$).

Kit was expressed by astrocytes and progenitors

Immunostaining for Kit showed numerous positive cells with subependymal localization (Fig. 3A), and the Kit immunoreactivity did not extend in the rostral migratory stream (data not shown). Under higher magnification, the Kit⁺ cells exhibited stellate morphology and were single cells not clusters (Fig. 3B). Kit did not co-label with βIII-tubulin (Fig. 3C), while it co-stained extensively with S100β (Fig. 3D, G). A small fraction of the Kit⁺ cells were double-labeled for Flt1 (Fig. 3E), and an even smaller population of Kit⁺ cells was positive for BrdU (Fig. 3F).

The expression in SVZa of the hematopoietic/angiogenic tyrosine kinase receptors Tie2 and Tie1, and the Tie2 ligands Ang-1 and -2 was restricted to endothelial cells (Fig. 3H–J).

The neurotrophins and their receptors in SVZa

Both the NGF (Fig. 4A) and BDNF (Fig. 4D) signals formed an immunopositive band of cells with subependymal localization, similarly to what observed for VEGF. NGF co-labeled with S100β (Fig. 4B) and with VEGF (Fig. 4C) but not with βIII-tubulin or BrdU (Fig. 4A, L). Similarly to NGF, BDNF exhibited a high percentage of co-labeling with S100β (Fig. 4D, M) but not with βIII-tubulin (Fig. 4E), and was also expressed in the rostral migratory stream (data

not shown). Both TrkA and TrkB co-labeled with S100β (Fig. 4F, N, O) and VEGF (Fig. 4I), but had a differential co-labeling pattern with BrdU and βIII-tubulin. TrkA was not expressed by the $BrdU^+$ clusters (Fig. 4G), while TrkB did co-stain with BrdU (Fig. 4H). TrkA was expressed in $\beta III\text{-tubulin}^+$ cells (Fig. 4J) while TrkB was not co-stained with βIII-tubulin (Fig. 4O). Both TrkA and TrkB were present in the rostral migratory stream. The expression of the pan-neurotrophin receptor p75 was restricted to blood vessels (Fig. 4K).

The NT3/TrkC and the GDNF/glial cell line-derived neurotrophic factor family receptor α1 (GFRα1) neurotrophin systems had a comparable SVZa distribution. Double-staining for NT3 and its high-affinity receptor TrkC showed a prominent signal at the ependymal border (Fig. 5A1) although subependymal cells were stained as well (Fig. 5A2, A3). Neither NT3 nor TrkC did co-stain with BrdU (Fig. 5B). NT3 co-labeled with S100β (Fig. 5C, H1), and VEGF (Fig. 5D, H1), the double-stained cells exhibiting stellate morphology (Fig. 5C, D; arrows) or being perivascular. Further, NT3 co-stained with subependymal cells positive for GFRα1, the glycosylphosphatidylinositol-anchored cell surface receptor of GDNF (Fig. 5E). Most of the $GFR\alpha1^+$ cells co-expressed S100β (Fig. 5H3), and a comparable percentage of $GFR\alpha1^+$ cells were co-labeled for VEGF (Fig. 5F, H3). A comparison of the expression of GFRα1 with that of its ligand GDNF revealed that the in contrast to GFRα1, the GDNF immunoreactivity was mainly localized to the ependymal cells (Fig. 5G). Both GDNF and GFRα1 were also positive in SVZa blood vessels (Fig. 5G2, 5G3; arrows). Ret, the transmembrane tyrosine kinase receptor of GDNF was not expressed in SVZa.

DISCUSSION

In this study, we provided structural evidence that several angiogenic and/or neurotrophic factor systems were expressed at protein level in adult monkey progenitor cell niche. These ligand/receptor systems might be involved in the *in vivo* regulation of primate progenitor cells, and thus could be a feasible target for manipulation in precursor cell-centered therapies in humans. Further, our data represent an attempt to construct molecular phenotypization of the cellular types in the monkeys SVZa niche in order to better understand their interrelationships.

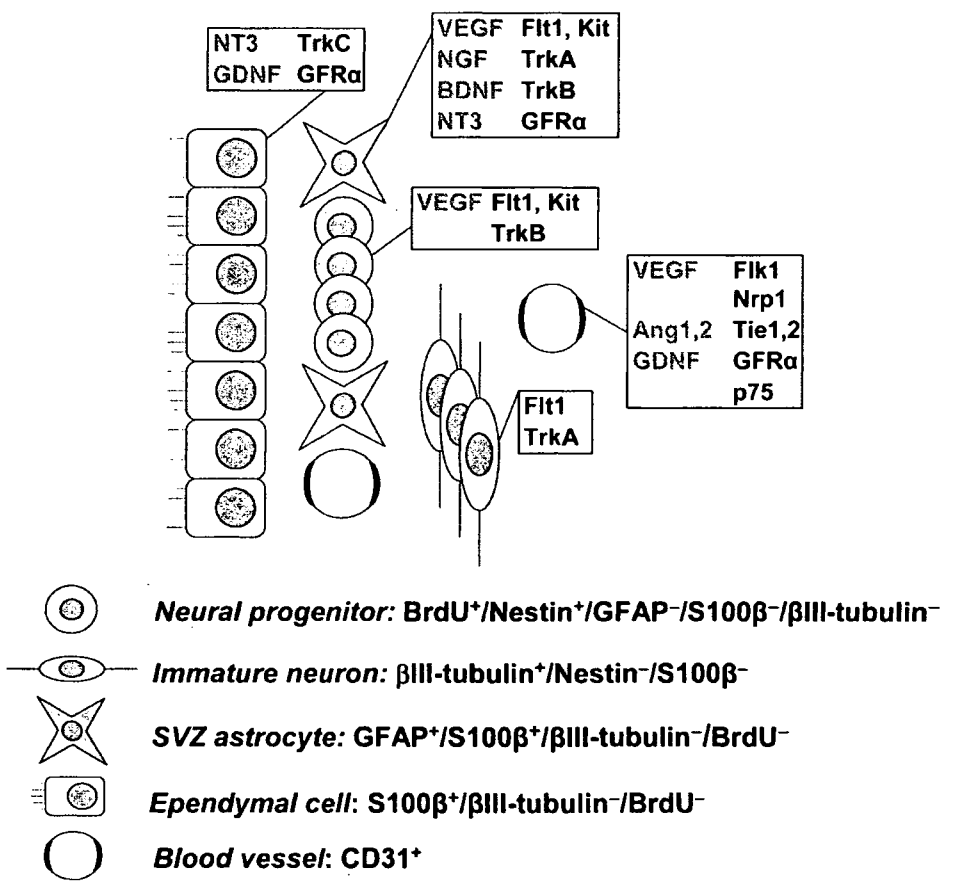

Fig. 6. Summary of ligand/receptor protein expression patterns by the major cell populations comprising monkey SVZa. Putative progenitor phenotypes are annotated in gray with their characteristic cell-selective marker combinations listed. Abbreviations: p75NTR, 75 kD pan-neurotrophin receptor.

We identified the characteristic expression pattern of angiogenic/neurotrophic signaling molecules and their receptors in five distinct cell types comprising the progenitor cell niche of adult monkey SVZa (Fig. 6). A link between blood vessels and neurogenesis is well appreciated in non-primate mammals (Leventhal et al., 1999; Palmer et al., 2000; Palmer, 2002; Louissaint et al., 2002; Shen et al., 2004; Wurmser et al., 2004), and begins to be unveiled in the monkey brain (Yamashima et al., 2004). The data presented in this study are in accordance with the view of a vascular signaling network involvement in primate progenitor cell regulation. Such a network could entail a neurotrophin–VEGF interplay, as $TrkA^+$ and $Flt1^+$ cells co-expressed VEGF, NGF and BDNF, opening a possibility for VEGF/neurotrophin paracrine or autocrine signaling (Calza et al., 2001; Louissaint et al., 2002; Fabel et al., 2003) in monkey SVZa. Further, SVZa astrocytes were positive for many of the molecules studied, and future studies are needed to delineate whether SVZa astrocytes are the principal progenitors in adult monkey SVZa (Sanai et al., 2004) or they are a non-progenitor cell type implicated in the regulation of the $BrdU^+$ precursors. Our results also suggest that ependyma-derived signals such as NT3 and GDNF could affect the subependymal niche cellular components in the monkey. In ischemic rodent brain, GDNF enhanced the SVZa progenitor neurogenesis (Kobayashi et al., 2006) via effects which do not appear to depend on the Ret tyrosine kinase (Arvidsson et al., 2001), consistent with the lack of Ret expression in SVZa in our monkey specimens. Thus, the operation of the GDNF system in SVZa may be exerted through GFRa1 and polysialylated neural cell adhesion molecule (PSA-NCAM) (Paratcha et al., 2006) signaling, or via additional transmembrane effectors (Pozas and Ibanez, 2005).

While the involvement of a vascular signaling network in the progenitor cell biology appears to be a conserved phenomenon between non-primate and primate mammals, interspecies molecular distinctions appear to exist. A major finding of the present study was the expression of the VEGF receptor Flt1 by proliferating progenitors of monkey SVZa, in contrast to the rodent SVZa where the major VEGF receptor expressed in the niche was Flk1 (Jin et al., 2002a). Notably, the Flt1-selective ligand VEGF-B also has pro-neurogenic effects in rodents (Sun et al., 2006), although of a significantly lower magnitude than the VEGF/Flk1-mediated effects (Jin et al., 2002a). The number of $Flt1^+/BrdU^+$ cells in monkey SVZa increased early after ischemia, while Flt1 was not present on the fraction of sustained progenitors remaining in SVZa for months after injury. These results suggest that Flt1 may be involved in the regulation of proliferation rather than differentiation of monkey precursor cells. Differential expression of Flt1, Flk1 and Nrp1 by primate or rodent precursors might be at least in part responsible for interspecies differences in progenitor cell biology (Sanai et al., 2004; Tonchev et al., 2003, 2005; Yamashima et al., 2004).

Deciphering the signaling regulating endogenous progenitor cell proliferation and differentiation in the primate brain is a requirement for developing effective cell replacement therapies in humans. The mere morphological finding of expression of a certain factor by a given cell type does not provide information on the function of this factor, and thus at present it remains unclear how the molecules investigated in our study would modulate monkey SVZa progenitors after ischemia or whether these factors are induced in response to the changes in the precursor cell proliferation and/or differentiation. Nevertheless, the results presented here are a step in determining the molecular "signature" of the cell types comprising monkey progenitor cell niche, and therefore may be helpful to more effectively design growth factor-based strategies for enhancement of endogenous precursor cells in monkey models, and eventually in the diseased human brain.

Acknowledgments—Research was sponsored by grants from the Japanese Ministries of Education, Culture, Sports, Science and Technology (Kiban B: 15390432) and Health, Labor and Welfare (H15-Kokoro-018), and the National Science Fund of Bulgaria (L1311/03). The technical expertise of Masaya Ueno is highly appreciated.

REFERENCES

Arvidsson A, Kokaia Z, Airaksinen MS, Saarma M, Lindvall O (2001) Stroke induces widespread changes of gene expression for glial cell line-derived neurotrophic factor family receptors in the adult rat brain. Neuroscience 106:27–41.

Arvidsson A, Collin T, Kirik D, Kokaia Z, Lindvall O (2002) Neuronal replacement from endogenous precursors in the adult brain after stroke. Nat Med 8:963–970.

Bedard A, Gravel C, Parent A (2006) Chemical characterization of newly generated neurons in the striatum of adult primates. Exp Brain Res 170:501–512.

Benraiss A, Chmielnicki E, Lerner K, Roh D, Goldman SA (2001) Adenoviral brain-derived neurotrophic factor induces both neostriatal and olfactory neuronal recruitment from endogenous progenitor cells in the adult forebrain. J Neurosci 21:6718–6731.

Calza L, Giardino L, Giuliani A, Aloe L, Levi-Montalcini R (2001) Nerve growth factor control of neuronal expression of angiogenetic and vasoactive factors. Proc Natl Acad Sci U S A 98:4160–4165.

Calza L, Giuliani A, Fernandez M, Pirondi S, D'Intino G, Aloe L, Giardino L (2003) Neural stem cells and cholinergic neurons: regulation by immunolesion and treatment with mitogens, retinoic acid, and nerve growth factor. Proc Natl Acad Sci U S A 100: 7325–7330.

Carmeliet P (2003) Blood vessels and nerves: common signals, pathways and diseases. Nat Rev Genet 4:710–720.

Chen Y, Ai Y, Slevin JR, Maley BE, Gash DM (2005) Progenitor proliferation in the adult hippocampus and substantia nigra induced by glial cell line-derived neurotrophic factor. Exp Neurol 196:87–95.

Dempsey RJ, Sailor KA, Bowen KK, Tureyen K, Vemuganti R (2003) Stroke-induced progenitor cell proliferation in adult spontaneously hypertensive rat brain: effect of exogenous IGF-1 and GDNF. J Neurochem 87:586–597.

Emanueli C, Schratzberger P, Kirchmair R, Madeddu P (2003) Paracrine control of vascularization and neurogenesis by neurotrophins. Br J Pharmacol 140:614–619.

Fabel K, Fabel K, Tam B, Kaufer D, Baiker A, Simmons N, Kuo CJ, Palmer TD (2003) VEGF is necessary for exercise-induced adult hippocampal neurogenesis. Eur J Neurosci 18:2803–2812.

Ferrara N, Gerber HP, LeCouter J (2003) The biology of VEGF and its receptors. Nat Med 9:669–676.

Ghosh A, Greenberg ME (1995) Distinct roles for bFGF and NT-3 in the regulation of cortical neurogenesis. Neuron 15:89–103.

Gougeon A, Busso D (2000) Morphologic and functional determinants of primordial and primary follicles in the monkey ovary. Mol Cell Endocrinol 163:33–42.

Hayashi M, Mitsunaga F, Itoh M, Shimizu K, Yamashita A (2000) Development of full-length Trk B-immunoreactive structures in the prefrontal and visual cortices of the macaque monkey. Anat Embryol (Berl) 201:139–147.

Hayashi M, Mistunaga F, Ohira K, Shimizu K (2001) Changes in BDNF-immunoreactive structures in the hippocampal formation of the aged macaque monkey. Brain Res 918:191–196.

Iwai M, Sato K, Kamada H, Omori N, Nagano I, Shoji M, Abe K (2003) Temporal profile of stem cell division, migration, and differentiation from subventricular zone to olfactory bulb after transient forebrain ischemia in gerbils. J Cereb Blood Flow Metab 23:331–341.

Jin K, Minami M, Lan JQ, Mao XO, Batteur S, Simon RP, Greenberg DA (2001) Neurogenesis in dentate subgranular zone and rostral subventricular zone after focal cerebral ischemia in the rat. Proc Natl Acad Sci U S A 98:4710–4715.

Jin K, Zhu Y, Sun Y, Mao XO, Xie L, Greenberg DA (2002a) Vascular endothelial growth factor (VEGF) stimulates neurogenesis in vitro and in vivo. Proc Natl Acad Sci U S A 99:11946–11950.

Jin K, Mao XO, Sun Y, Xie L, Greenberg DA (2002b) Stem cell factor stimulates neurogenesis in vitro and in vivo. J Clin Invest 110:311–319.

Kawada H, Takizawa S, Takanashi T, Morita Y, Fujita J, Fukuda K, Takagi S, Okano H, Ando K, Hotta T (2006) Administration of hematopoietic cytokines in the subacute phase after cerebral infarction is effective for functional recovery facilitating proliferation of intrinsic neural stem/progenitor cells and transition of bone marrow-derived neuronal cells. Circulation 113:701–710.

Kim H, Li Q, Hempstead BL, Madri JA (2004) Paracrine and autocrine functions of brain-derived neurotrophic factor (BDNF) and nerve growth factor (NGF) in brain-derived endothelial cells. J Biol Chem 279:33538–33546.

Kobayashi T, Ahlenius H, Thored P, Kobayashi R, Kokaia Z, Lindvall O (2006) Intracerebral infusion of glial cell line-derived neurotrophic factor promotes striatal neurogenesis after stroke in adult rats. Stroke 37:2361–2367.

Kornack DR, Rakic P (2001) The generation, migration, and differentiation of olfactory neurons in the adult primate brain. Proc Natl Acad Sci U S A 98:4752–4757.

Leventhal C, Rafii S, Rafii D, Shahar A, Goldman SA (1999) Endothelial trophic support of neuronal production and recruitment from the adult mammalian subependyma. Mol Cell Neurosci 13:450–464.

Lewis Carl SA, Gillete-Ferguson I, Ferguson DG (1993) An indirect immunofluorescence procedure for staining the same cryosection with two mouse monoclonal primary antibodies. J Histochem Cytochem 41:1273–1278.

Li TS, Hamano K, Nishida M, Hayashi M, Ito H, Mikamo A, Matsuzaki M (2003) CD117+ stem cells play a key role in therapeutic angiogenesis induced by bone marrow cell implantation. Am J Physiol Heart Circ Physiol 285:H931–H937.

Lichtenwalner RJ, Parent JM (2006) Adult neurogenesis and the ischemic forebrain. J Cereb Blood Flow Metab 26:1–20.

Lledo PM, Alonso M, Grubb MS (2006) Adult neurogenesis and functional plasticity in neuronal circuits. Nat Rev Neurosci 7:179–193.

Louissaint A Jr, Rao S, Leventhal C, Goldman SA (2002) Coordinated interaction of neurogenesis and angiogenesis in the adult songbird brain. Neuron 34:945–960.

Muzio L, DiBenedetto B, Stoykova A, Boncinelli E, Gruss P, Mallamaci A (2002) Conversion of cerebral cortex into basal ganglia in Emx2(-/-) Pax6(Sey/Sey) double-mutant mice. Nat Neurosci 5: 737–745.

Okano H (2002) The stem cell biology of the central nervous system. J Neurosci Res 69:698–707.

Otani A, Takagi H, Oh H, Koyama S, Matsumura M, Honda Y (1999) Expressions of angiopoietins and Tie2 in human choroidal neovascular membranes. Invest Ophthalmol Vis Sci 40:1912–1920.

Palmer TD, Willhoite AR, Gage FH (2000) Vascular niche for adult hippocampal neurogenesis. J Comp Neurol 425:479–494.

Palmer TD (2002) Adult neurogenesis and the vascular Nietzsche. Neuron 34:856–858.

Paratcha G, Ibanez CF, Ledda F (2006) GDNF is a chemoattractant factor for neuronal precursor cells in the rostral migratory stream. Mol Cell Neurosci 31:505–514.

Parent JM, Vexler ZS, Gong C, Derugin N, Ferriero DM (2002) Rat forebrain neurogenesis and striatal neuron replacement after focal stroke. Ann Neurol 52:802–813.

Parikh AA, Fan F, Liu WB, Ahmad SA, Stoeltzing O, Reinmuth N, Bielenberg D, Bucana CD, Klagsbrun M, Ellis LM (2004) Neuropilin-1 in human colon cancer: expression, regulation, and role in induction of angiogenesis. Am J Pathol 164:2139–2151.

Pencea V, Bingaman KD, Freedman LJ, Luskin MB (2001a) Neurogenesis in the subventricular zone and rostral migratory stream of the neonatal and adult primate forebrain. Exp Neurol 172:1–16.

Pencea V, Bingaman KD, Wiegand SJ, Luskin MB (2001b) Infusion of brain-derived neurotrophic factor into the lateral ventricle of the adult rat leads to new neurons in the parenchyma of the striatum, septum, thalamus, and hypothalamus. J Neurosci 21:6706–6717.

Pincus DW, Keyoung HM, Harrison-Restelli C, Goodman RR, Fraser RA, Edgar M, Sakakibara S, Okano H, Nedergaard M, Goldman SA (1998) Fibroblast growth factor-2/brain-derived neurotrophic factor-associated maturation of new neurons generated from adult human subependymal cells. Ann Neurol 43:576–585.

Pozas E, Ibanez CF (2005) GDNF and GFRalpha1 promote differentiation and tangential migration of cortical GABAergic neurons. Neuron 45:701–713.

Quartu M, Lai ML, Del Fiacco M (1999) Neurotrophin-like immunoreactivity in the human hippocampal formation. Brain Res Bull 48:375–382.

Quartu M, Serra MP, Manca A, Follesa P, Ambu R, Del Fiacco M (2003) High affinity neurotrophin receptors in the human pre-term newborn, infant, and adult cerebellum. Int J Dev Neurosci 21:309–320.

Ruef J, Hu ZY, Yin LY, Wu Y, Hanson SR, Kelly AB, Harker LA, Rao GN, Runge MS, Patterson C (1997) Induction of vascular endothelial growth factor in balloon-injured baboon arteries. A novel role for reactive oxygen species in atherosclerosis. Circ Res 81:24–33.

Sanai N, Tramontin AD, Quinones-Hinojosa A, Barbaro NM, Gupta N, Kunwar S, Lawton MT, McDermott MW, Parsa AT, Manuel-Garcia Verdugo J, Berger MS, Alvarez-Buylla A (2004) Unique astrocyte ribbon in adult human brain contains neural stem cells but lacks chain migration. Nature 427:740–744.

Sandell JH, Baker LS Jr, Davidov T (1998) The distribution of neurotrophin receptor TrkC-like immunoreactive fibers and varicosities in the rhesus monkey brain. Neuroscience 86:1181–1194.

Serra MP, Quartu M, Ambu R, Follesa P, Del Fiacco M (2002) Immunohistochemical localization of GDNF in the human hippocampal formation from prenatal life to adulthood. Brain Res 928:138–146.

Serra MP, Quartu M, Mascia F, Manca A, Boi M, Pisu MG, Lai ML, Del Fiacco M (2005) Ret, GFRalpha-1, GFRalpha-2 and GFRalpha-3 receptors in the human hippocampus and fascia dentata. Int J Dev Neurosci 23:425–438.

Shen Q, Goderie SK, Jin L, Karanth N, Sun Y, Abramova N, Vincent P, Pumiglia K, Temple S (2004) Endothelial cells stimulate self-renewal and expand neurogenesis of neural stem cells. Science 304:1338–1340.

Sun Y, Jin K, Xie L, Childs J, Mao XO, Logvinova A, Greenberg DA (2003) VEGF-induced neuroprotection, neurogenesis, and angiogenesis after focal cerebral ischemia. J Clin Invest 111:1843–1851.

Sun Y, Jin K, Childs JT, Xie L, Mao XO, Greenberg DA (2006) Vascular endothelial growth factor-B (VEGFB) stimulates

neurogenesis: evidence from knockout mice and growth factor administration. Dev Biol 289:329–335.

Tissot van Patot MC, Bendrick-Peart J, Beckey VE, Serkova N, Zwerdlinger L (2004) Greater vascularity, lowered HIF-1/DNA binding, and elevated GSH as markers of adaptation to in vivo chronic hypoxia. Am J Physiol Lung Cell Mol Physiol 287:L525–L532.

Tonchev AB, Yamashima T, Zhao L, Okano HJ, Okano H (2003) Proliferation of neural and neuronal progenitors after global brain ischemia in young adult macaque monkeys. Mol Cell Neurosci 23:292–301.

Tonchev AB, Yamashima T, Sawamoto K, Okano H (2005) Enhanced proliferation of progenitor cells in the subventricular zone and limited neuronal production in the striatum and neocortex of adult macaque monkeys after global cerebral ischemia. J Neurosci Res 81:776–788.

Uchida T, Nakashima M, Hirota Y, Miyazaki Y, Tsukazaki T, Shindo H (2000) Immunohistochemical localisation of protein tyrosine kinase receptors Tie-1 and Tie-2 in synovial tissue of rheumatoid arthritis: correlation with angiogenesis and synovial proliferation. Ann Rheum Dis 59:607–614.

Walker DG, Beach TG, Xu R, Lile J, Beck KD, McGeer EG, McGeer PL (1998) Expression of the proto-oncogene Ret, a component of the GDNF receptor complex, persists in human substantia nigra neurons in Parkinson's disease. Brain Res 79:207–217.

Wurmser AE, Palmer TD, Gage FH (2004) Neuroscience. Cellular interactions in the stem cell niche. Science 304:1253–1255.

Yamashima T, Kohda Y, Tsuchiya K, Ueno T, Yamashita J, Yoshioka T, Kominami E (1998) Inhibition of ischaemic hippocampal neuronal death in primates with cathepsin B inhibitor CA-074: a novel strategy for neuroprotection based on "calpain-cathepsin hypothesis." Eur J Neurosci 10:1723–1733.

Yamashima T, Tonchev AB, Vachkov IH, Popivanova BK, Seki T, Sawamoto K, Okano H (2004) Vascular adventitia generates neuronal progenitors in the monkey hippocampus after ischemia. Hippocampus 14:861–875.

Zhang RL, Zhang ZG, Zhang L, Chopp M (2001) Proliferation and differentiation of progenitor cells in the cortex and the subventricular zone in the adult rat after focal cerebral ischemia. Neuroscience 105:33–41.

Zhang H, Vutskits L, Pepper MS, Kiss JZ (2003) VEGF is a chemoattractant for FGF-2-stimulated neural progenitors. J Cell Biol 163:1375–1384.

Zhang RL, Zhang ZG, Chopp M (2005) Neurogenesis in the adult ischemic brain: generation, migration, survival, and restorative therapy. Neuroscientist 11:408–416.

APPENDIX

Supplementary data

Supplementary data associated with this article can be found, in the online version, at doi: 10.1016/j.neuroscience.2006.10.052.

(Accepted 23 October 2006)
(Available online 22 December 2006)

Inhibition of axonal outgrowth in the tumor environment: Involvement of class 3 semaphorins

Ivan H. Vachkov,[1,2] Xiaoyong Huang,[1,3] Yoshihiro Yamada,[1,3] Anton B. Tonchev,[4] Tetsumori Yamashima,[5] Satoru Kato[2] and Nobuyuki Takakura[1,3,6]

Departments of [1]Stem Cell Biology, Cancer Research Institute, [2]Molecular Neurobiology, Graduate School of Medical Science, Kanazawa University, Kanazawa 920-8640; [3]Department of Signal Transduction, Research Institute for Microbial Diseases, Osaka University, 3-1 Yamada-oka, Suita, Osaka 565-0871; [4]Department of Cell Biology, Division of Forensic Medicine, Varna Medical University, Varna, Bulgaria; [5]Department of Restorative Neurosurgery, Graduate School of Medical Science, Kanazawa University, Takara-machi 13-1, Kanazawa, 920-8641, Japan

(Received December 21, 2006/Revised April 3, 2007/Accepted April 6, 2007/Online publication May 14, 2007)

That tumors lack innervation is dogma in the field of pathology, but the molecular determinants of this phenomenon remain elusive. We studied the effects of conditioned media from Colon 26 and B16 mouse tumor cell lines on the axonal outgrowth and cellular differentiation of embryonic Institute of Cancer Research (ICR) mouse dorsal root ganglion cells. Tumor-conditioned media suppressed dorsal root ganglion axonal extension but had no effect on neuronal or glial differentiation. We found that the tumor cells expressed most of the class 3 semaphorins – axon guidance molecules. Blocking the activity of class 3 semaphorins with the soluble receptor neuropilin-1 significantly counteracted the tumor-induced inhibition of axonal extension. Together, these results suggest a role for tumor-secreted class 3 semaphorins in selectively inhibiting axonal outgrowth of dorsal root ganglion neurons. (*Cancer Sci* 2007; 98: 1192–1197)

The lack of innervation in tumors is a generally accepted fact,[1] but the molecular determinants of this phenomenon are poorly understood. Furthermore, certain tumors such as esophageal cancer were shown to be innervated by peptidergic nerve fibers and to promote process extension in DRG neurons.[2] Notably, sarcomas can secrete NGF, which promotes proliferation and axonal outgrowth of DRG neurons, the observation of which led to the initial discovery of NGF.[3] Thus, the effects of tumors on axonal growth are unclear and need further analysis.

Peripheral nerves are known to associate with blood vessels,[4] reflecting their need for oxygen and nutrients and their control of vasoconstriction and vasodilation.[5] In mutant embryos containing disorganized nerves, blood vessel branching is altered to follow the nerve,[6] suggesting that local signals supplied by nerve fibers may provide a template that determines blood vessel patterning. These data indicate a functional relationship between axonal outgrowth and angiogenesis under physiological conditions, and make the question of tumor innervation even more intriguing.

DRG neurons innervate most of the internal organs, thus their processes have the highest potential for interacting with the cells of a tumor growing in the body. We therefore investigated whether molecular cues secreted from tumor cells affect axonal outgrowth and additionally alter the differentiation capacity of immature neural cells in the DRG. Here, we report that supernatant isolated from two tumor cell line cultures inhibited process extension of DRG neurons, and present evidence implicating secreted class 3 semaphorins as mediators of this tumor-induced axonal inhibition.

Materials and Methods

DRG culture. Embryos at embryonic day 12.5 were dissected from pregnant Institute of Cancer Research (ICR) mice (SCL, Shizuoka, Japan). DRG were extracted free of surrounding tissues and placed one per well in 24-well, poly-L-lysine-coated culture plates (Iwaki, Tokyo, Japan). Colon 26 (C26; mouse colon cancer) and B16 (mouse melanoma) tumor cell lines were cultured in DMEM (Sigma-Aldrich, St Louis, MO, USA) supplemented with 10% FBS (Sigma-Aldrich). Culture supernatants were collected when cells reached approximately 80% confluence. Four culture media were prepared: (i) control medium, DMEM + 10% FBS + 50 ng/mL human recombinant NGF (PeproTech, Rocky Hill, NJ, USA); (ii) tumor-conditioned medium, equal amounts of control medium with 100 ng/mL NGF and tumor cell line supernatant were mixed; (iii) rescue medium, tumor-conditioned medium with 50 μg/mL recombinant fusion protein of the extracellular domain of murine Npn1 with the Fc fragment of human IgG; and (iv) control rescue medium, tumor-conditioned medium with 50 μg/mL recombinant fusion protein of the CD4 glycoprotein with the Fc fragment of human IgG.[7,8] DRG were incubated in one of the above media for 48 h and then fixed and stained. Culture media were replaced with fresh media after 24 h of incubation.

Immunocytochemistry. The immunohistochemical procedures on culture plates were basically the same as reported previously.[9] Briefly, DRG on culture plates were fixed in 4% paraformaldehyde in PBS (pH 7.5) for 10 min at RT and rinsed with PBST. Non-specific binding of secondary antibody was blocked with 5% normal goat serum and 1% bovine serum albumin in PBST (blocking serum) for 30 min at RT. Cultures were incubated with mouse anti-β-III tubulin primary antibody (1:200; Covance, Richmond, CA, USA) or rabbit anti-GFAP antibody (1:200; DAKO, Kyoto, Japan) overnight at 4°C in blocking serum, rinsed three times for 10 min at RT with PBST and then incubated with goat antimouse IgG conjugated to Alexa Fluor 488 (1:100; Invitrogen, Carlsbad, CA, USA) in blocking serum for 1 h at RT. Cultures were rinsed again with PBST, and PI was added for 1 min at RT for visualization of nuclei.

RT-PCR. Total RNA was isolated from C26, B16, LLC, cloneM-3 (mouse melanoma) and MM102-TC (mouse mammary gland carcinoma) cells using the Isogen (Wako, Osaka, Japan) isolation kit according to the manufacturer's instructions, and were reverse-transcribed with the SuperScript (Invitrogen) RT-PCR system as reported previously.[10] The class 3 semaphorin Npn1

[6]To whom correspondence should be addressed.
E-mail: ntakaku@biken.osaka-u.ac.jp
This work was mainly carried out at Kanazawa University.
Abbreviations: DMEM, Dulbecco's modified Eagle's medium; DRG, dorsal root ganglion; FBS, fetal bovine serum; GFAP, glial fibrillary acidic protein; LLC, Lewis lung carcinoma; NGF, nerve growth factor; Npn, neuropilin; PBS, phosphate-buffered saline; PBST, PBS–Triton X-100; PI, propidium iodide; RT, room temperature; RT-PCR, reverse transcription–polymerase chain reaction; Sema3, semaphorin-3; VEGF, vascular endothelial growth factor.

doi: 10.1111/j.1349-7006.2007.00508.x

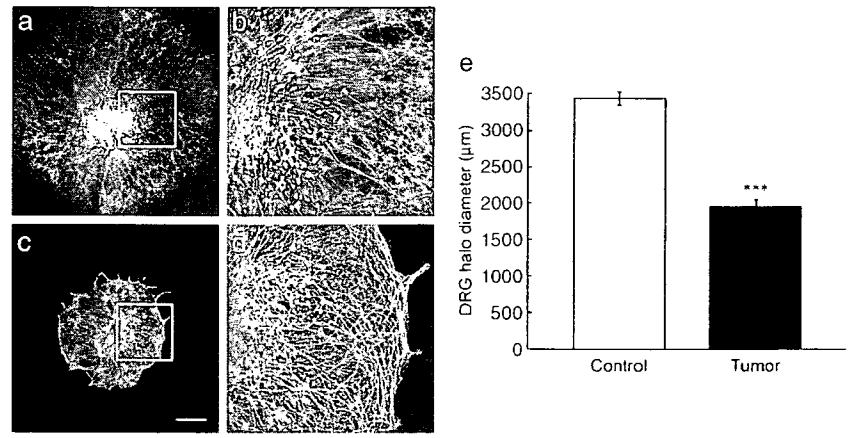

Fig. 1. Tumor-conditioned medium inhibits dorsal root ganglion (DRG) axonal outgrowth. Confocal images of DRG primary cultures exposed to (a,b) control medium or (c,d) colon 26 tumor-conditioned medium. Cultured cells were stained with anti-β-III tubulin antibody. (b,d) High-power views of areas indicated by boxes in (a) and (c), respectively. Scale bar = 500 μm. (e) Statistical evaluation of the DRG halo diameter. Data show mean ± SEM from five random fields. $*P < 0.001$ versus control. Shown are representative data from one of three independent experiments.

and Npn2, and β-actin gene sequences were amplified using ExTaq (TaKaRa, Tokyo, Japan) DNA polymerase with: Sema3A forward, 5′-CGGGACTTCGCTATCTTCAG-3′ and reverse, 5′-GGGACCATCTCTGTGAGCAT-3′; Sema3B forward, 5′-AACCC-ATGCTTCAACTGGAC-3′ and reverse, 5′-CTGGAGGTGGAG-AAGACAGC-3′; Sema3C forward, 5′-TGGCCACTCTTGC-TCTAGGT-3′ and reverse, 5′-GCCTTCAGCTTGCCATAGTC-3′; Sema3D forward, 5′-AGCACCGACCTTCAAGAGAA-3′ and reverse, 5′-GTGCATATCTGGAGCAAGCA-3′; Sema3E forward, 5′-TTGGACAGCAATTTGTTGGA-3′ and reverse, 5′-AGCCA-ATCAGCTGCAAGAAT-3′; Sema-3F forward, 5′-TGCTTGTC-ACTGCCTTCATC-3′ and reverse, 5′-TACAGGTGTGTTCGGT-TCCA-3′; Sema3G forward, 5′-TCTTTGGCACAGAGCACAAC-3′ and reverse, 5′-CCTGCACCATACACGTTCAC-3′; Npn1 forward, 5′-CTCCCGCCTGAACTACCCTGAAAAT-3′ and reverse, 5′-CCACTTGGAGCCATTCATTGGTGTA-3′; Npn2 forward, 5′-TGAATCTCCAGGGTTTCCAG-3′ and reverse, 5′-GTCCACCTCCCATCAGAGAA-3′; and β-actin forward, 5′-CCTAAGGCCAACCGTGAAAAG-3′ and reverse, 5′-TCTTC-ATGGTGCTAGGAGCAG-3′ primer pairs. The PCR products were fractioned by electrophoresis and the positive bands were visualized in a FAS III (Toyobo, Osaka, Japan) ultraviolet transilluminator.

Western blotting. C26 and B16 cells were trypsinized and collected. Procedures for the preparation of cell lysates and western blotting were basically the same as those reported previously.[11] Briefly, total protein was extracted using Nonidet (N)P-40 Tris buffer with proteinase inhibitor cocktail added. Proteins were fractioned by sodium dodecylsulfate–polyacrylamide gel electrophoresis and transferred to a membrane. The membrane was incubated for 30 min at RT with a generic protein to cover any remaining sticky places. Primary antibodies against mouse Sema3A (1:1000; Abcam, Cambridge, UK), Sema3C (1:1000; R&D Systems, Minneapolis, MN, USA) or glyceraldehyde-3-phosphate dehydrogenase (1:1000; Chemicon, Temecula, CA, USA) were added for 1 h at RT followed by horseradish peroxidase (HRP)-conjugated goat antimouse IgG (1:1000; DAKO). The positive bands were visualized by ECL detection reagents (Amersham Biosciences, Piscataway, NJ, USA) in a LAS-3000 imaging system (Fujifilm, Tokyo, Japan).

Image analysis. Single and double labeling were visualized by confocal laser scanning microscopy (LSM 510; Carl Zeiss, Göttingen, Germany). Alexa Fluor 488 was assigned to the green channel and PI to the red channel. For single-labeling experiments, an average of 16 z-axis scans was used to generate the final images. In double-labeling experiments, each fluorochrome was scanned separately and sequentially to minimize the probability of signal transfer among channels. Measurements of DRG halo diameter were carried out using Zeiss LSM software version 3.2 on six samples from each experimental group. Within each experimental group, at least 100 PI-positive cells were investigated for costaining with β-III tubilin or GFAP. Diameters and percentages of positive cells were averaged to obtain a mean density for each marker per experimental group.

Statistical analysis. Diameters of DRG halos were compared using Student's paired *t*-test. Percentages of cells expressing β-III tubulin or GFAP were compared using non-parametric tests (Mann–Whitney *U*-test and Kruskal–Wallis test). Data are expressed as mean ± SEM. Differences were considered significant when $P < 0.05$.

Results

Tumor-conditioned medium inhibited DRG axonal outgrowth. DRG cells cultured under normal conditions (control medium) grew steadily, and within 48 h of culturing extended radial processes in all directions (Fig. 1a,b), in agreement with previous studies using similar culture media (DMEM supplemented with NGF).[12,13] The removal of NGF from the culture medium resulted in extensive cell death (data not shown); therefore, all culture media were supplemented with NGF. In contrast, the DRG cells cultured with C26 (Fig. 1c) or B16 (Suppl. Fig. 1) tumor-conditioned medium showed limited axonal outgrowth and their axons lacked the straightness of control axons (Fig. 1d). Quantitative measurement of DRG halo diameters revealed that DRG cells grown in tumor-conditioned medium had significantly smaller halos than those grown in control medium (Fig. 1e).

Tumor-conditioned medium did not alter DRG cellular differentiation. Tumor-conditioned medium affected axonal outgrowth; however, tumor-conditioned medium may also be involved in other cellular processes such as differentiation of DRG cells. Therefore, we stained DRG cells cultured in control or tumor-conditioned media with antibodies against the neuronal marker β-III tubulin or the astrocyte marker GFAP; the nuclei of all cells were counterstained with the DNA-binding dye PI (Fig. 2a–l). We then quantitatively evaluated the percentages of β-III tubulin- or GFAP-positive cells among the total population of PI-stained cells under high magnification (Fig. 2m,n). We evaluated β-III tubulin-positive neuronal cells adjacent to the center of the DRG halo because the density of neuronal cells in the center was too high to clearly distinguish individual cells, but we evaluated GFAP-labeled astrocyte lineage cells in the periphery of the DRG halo where the incidence of astrocytes was high. The β-III tubulin-positive cells in both control (Fig. 2a–c) and tumor-conditioned media (Fig. 2d–f) had similar appearance, and quantitative analysis of the percentage of β-III tubulin-positive cells revealed that there was no significant difference between the control and tumor conditions (Fig. 2m). Likewise, the GFAP-positive cells in both control (Fig. 2g–i)

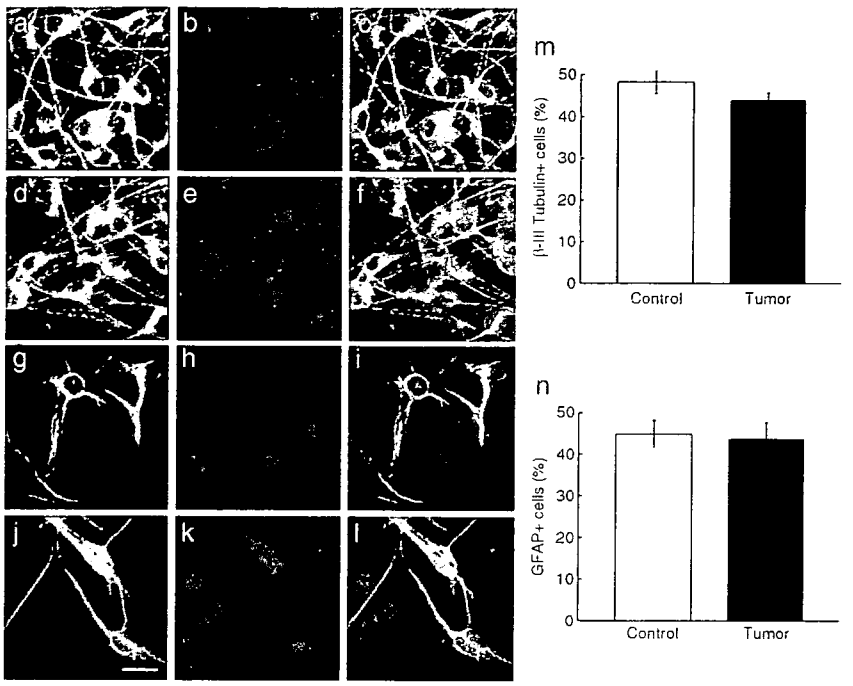

Fig. 2. Tumor-conditioned medium does not affect neuronal or glial differentiation of dorsal root ganglion (DRG) cells. Neuronal or glial cell development of DRG cells in primary cultures exposed to (a–c, g–i) control medium or (d–f, j–l) colon 26 tumor-conditioned medium was analyzed by staining for (a,d) the neuronal marker β-III tubulin or (g,j) the astrocyte marker glial fibrillary acidic protein (GFAP). Cells in (a,d,g,j) were counterstained with propidium iodide (PI) (b,e,h,k, respectively). The images in (c,f,i,l) are merged images of (a,b), (d,e), (g,h) and (j,k). Scale bar = 20 μm. (m,n) Percentage of β-III tubulin-positive neuronal cells (m) or GFAP-positive glial cells (n) among the total PI-positive cells in DRG primary cultures exposed to control or colon 26 tumor-conditioned medium. Data are mean ± SEM from five random fields. Shown are representative data from one of three independent experiments.

and tumor-conditioned media (Fig. 2j–l) had similar appearances, and there were no significant differences in the percentage of astroglial cells in the two conditions (Fig. 2n). Together, these results indicate that suppression of DRG axonal outgrowth in tumor-conditioned medium did not result from an altered differentiation of the DRG cells into neuronal and astrocyte lineages.

Effects of tumor-conditioned medium on DRG were dependent on class3 semaphorins. Based on the above results, we searched for molecular cues in the tumor-conditioned medium that potentially inhibit axonal outgrowth from DRG cells. Due to its well-known growth cone repulsive effects,[14–17] and because it is the only secreted class of the semaphorin family of proteins in vertebrates,[18] we examined class 3 semaphorin expression in C26 and B16 tumor cells. We found that both C26 and B16 cells expressed Sema3A, Sema3B, Sema3C, Sema3D, Sema3E and Sema3F mRNA (Fig. 3a). Moreover, we found that other cancer cell lines, such as LLC, cloneM-3 (mouse melanoma) and MM102-TC (mouse mammary gland carcinoma) also express several class 3 semaphorins. Interestingly, the tumor cells we observed expressed more or less either Npn1 or Npn2, receptors for class 3 semaphorins. Further, western blotting of tumor cell revealed the presence of Sema3A and Sema3C proteins from both Colon26 and B16 cells (Fig. 3b).

As class 3 semaphorins are soluble ligands for Npn1, we tried to inactivate the function of Sema3 in the cultures. For this purpose we generated a recombinant fusion protein (Npn1–Fc) of the extracellular domain of murine Npn1 and the Fc fragment of human IgG.[7,8] In the presence of Npn1-Fc (50 μg/mL), DRG cells cultured in C26 tumor-conditioned medium (Fig. 4e,f) appeared to show more extensive axonal outgrowth than those cultured in C26 tumor-conditioned medium containing the CD4-Fc control protein (Fig. 4c,d), but less than those cultured in control medium (Fig. 4a,b). Morphometric analyses confirmed this impression, as the DRG halo diameters in C26 tumor-conditioned media with Npn1-Fc were significantly larger than those in C26 tumor-conditioned media alone, but still significantly smaller than that with control medium (Fig. 4g). A lower concentration of Npn1-Fc (10 μg/mL) produced results that were not significantly

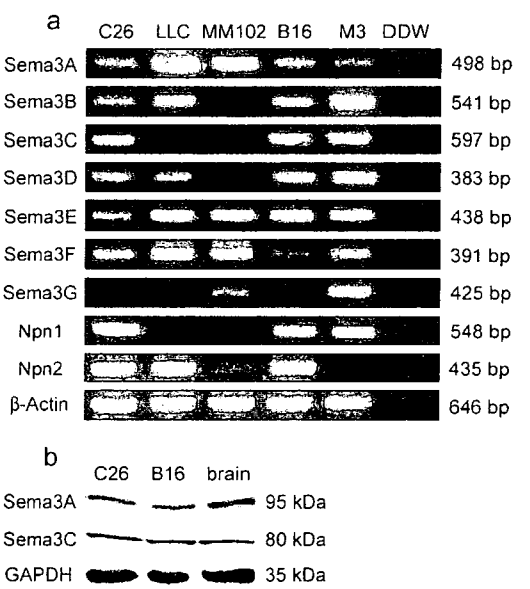

Fig. 3. Tumor cell lines express class 3 semaphorins. (a) Reverse transcription–polymerase chain reaction analysis of mRNA extracted from colon 26 (C26) cells, B16 cells, lewis lung carcinoma (LLC), cloneM-3 (mouse melanoma) and MM102-TC (mouse mammary gland carcinoma). Distilled water was used as a negative control. Non-reverse transcribed RNA did not generate any polymerase chain reaction product. β-Actin was used as an internal loading control. (b) Western blotting of C26 and B16 cells. Glyceraldehyde-3-phosphate was used as an internal control.

different from those in the C26 tumor-conditioned medium, and an excess of the Npn1-Fc (250 μg/mL) did not add to its rescue effects for axonal outgrowth (Fig. 4g). As observed in the effect of Npn1-Fc for C26 tumor-conditioned media, in the presence of Npn1-Fc DRG cells cultured in B16 tumor-conditioned

doi: 10.1111/j.1349-7006.2007.00508.x

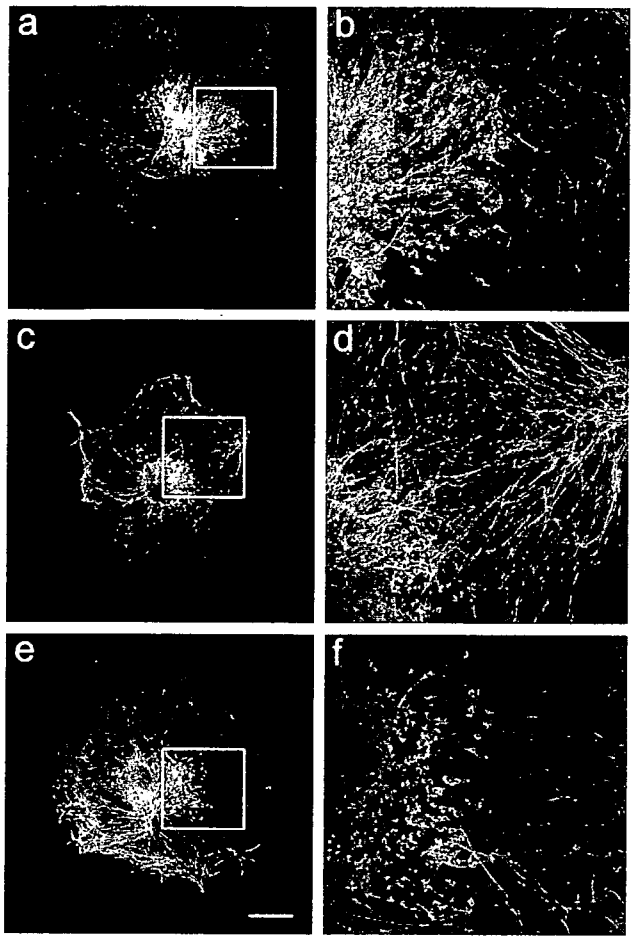

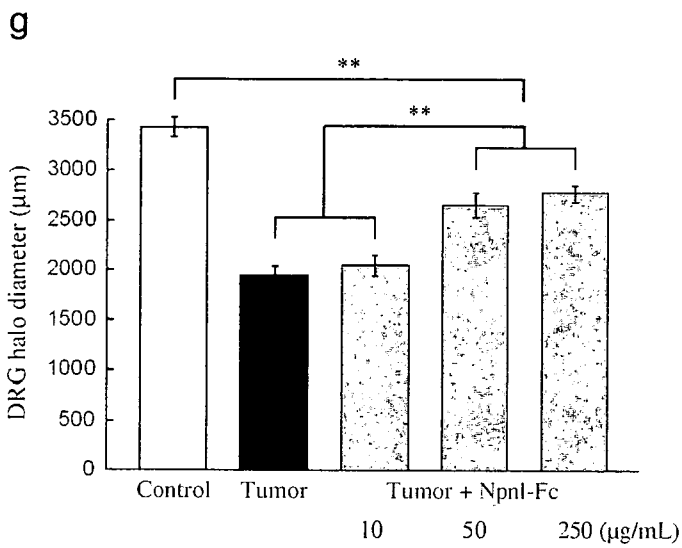

Fig. 4. Inactivation of class 3 semaphorins rescues dorsal root ganglion (DRG) axonal outgrowth. Confocal images of (a,b) DRG primary cultures grown in control medium, (c,d) colon 26 tumor-conditioned medium with CD4-Fc control protein, or (e,f) colon 26 tumor-conditioned medium with 50 μg/mL neuropilin-1-Fc protein. Cultured cells were stained with anti-β-III tubulin antibody. (b,d,f) High-power views of the areas indicated by boxes in (a,c,e). Scale bar = 500 μm. (g) Quantitative evaluation of the DRG halo diameter. Control, control medium; tumor, colon 26 tumor-conditioned medium. Data show mean ± SEM from five random fields. Shown are representative data from one of three independent experiments. $*P < 0.01$.

medium appeared to exhibit more extensive axonal outgrowth than those cultured in B16 tumor-conditioned medium containing the CD4-Fc control protein (Suppl. Fig. 1).

Discussion

The nervous and vascular systems share several anatomical parallels and both systems utilize a complex branching network of neuronal cells or blood vessels to control all regions of the body. From the anatomical and juxtapositional similarities of the nervous and vascular systems, it has been suggested that axons might guide blood vessels, and vice versa. Indeed, VEGF (or VEGF-A) from neuronal cells guides blood vessels,[6] and signals from vessels, such as artemin and neurotrophin 3, attract axons to track alongside the vessel.[19,20] In this manner, the neuronal and vascular systems are coordinately well organized in normal tissues; however, in tumor tissues, with a few exceptions, little innervation is observed. In adulthood, regenerated tissue responding to tissue damage is reinnervated along with angiogenesis. Although angiogenesis is commonly observed in the tumor environment and regenerated normal tissue area, why innervation does not occur in the tumor environment has not been elucidated at the molecular level. In the present study, we found one candidate that inhibits innervation in tumors, class 3 semaphorins, molecules well known to induce repulsion of axons.[15–18]

A series of genetic and biochemical screens identified proteins acting in an instructive manner to actively attract or repel axons, and four types of molecules relating to axon guidance have been isolated, including members of the semaphorin, ephrin, netrin and slit families.[21] In the present study, it was clear that soluble factors inhibited axon outgrowth because we used the culture supernatant of tumor cells to examine outgrowth in cultured DRG cells. Therefore, among the four kinds of axon guidance molecules described above, we excluded the ephrin family because they are membrane proteins.[22] Moreover, two of the other families of molecules, netrins and slits, function as both attractive and repulsive cues to axons depending on their concentrations in the foci, and originally attract commissural axons to the midline of the brain.[21] Conversely, several papers have reported semaphorin expression associated with tumor angiogenesis in the tumor environment.[23,24] Based on this evidence, we examined semaphorin expression in tumor cells.

Semaphorins are a large family of signaling proteins, both secreted and membrane bound. They are divided into eight classes. Among these, class 3 semaphorins (Sema3A–G) are the only secreted forms in vertebrates. Moreover, all class 3 semaphorins were shown to be chemorepulsive for many class of axons, and so far Sema3A, Sema3C, Sema3D and Sema3E were found to bind Npn1 with high affinity.[23] Among the class 3 semaphorins, Sema3A has been most intensively studied in relation to axon guidance.[15–18] Sema3A shows repulsive activity toward a variety of neuronal types, including motor, sensory, olfactory and hippocampal neurons.[25–30] Npn1 and Npn2 were the first receptors identified for Sema3A.[31,32] The transmembrane protein Npn1 forms a homodimer receptor complex for Sema3A. Mice lacking Npn1 have a similar phenotype to those lacking Sema3A, namely, marked defasciculation of nerve bundles and aberrant projections of sensory nerves.[33,34] Although Npn1 itself does not contain a kinase domain or binding site of the adaptor protein for signal transduction in the cytoplasmic domain, together with plexins it forms a functional receptor complex to induce signals into cells.[13,35] In this way, Sema3A was studied extensively and is suggested to induce strong chemorepulsion for almost all axons. Therefore, we first tried to knockdown the *Sema3A* gene in C26 and B16 tumor cells, with Sema3A-depleted C26 or B16 tumor-conditioned media being used in DRG culture. However, merely depletion of Sema3A from tumor-conditioned

media did not alter tumor-conditioned media-mediated inhibition of axon outgrowth from DRG (data not shown). Consistent with the result of the *Sema3A* knockdown, our present data showed that almost all class 3 semaphorins were produced from tumor cells, and that soluble Npn1 protein rescued axon outgrowth resulting from tumor-conditioned media. Therefore, we confirm that class 3 semaphorins derived from tumor cells are involved in the inhibition of axon outgrowth. However, soluble Npn1 did not completely rescue the extension of axons to the control level. It is possible that other secreted molecules, including some members of class 3 semaphorins, bind to Npn2 alone. Moreover, in the present study, we focused on soluble proteins for axon extension; however, axon outgrowth is controlled not only by secreted factors but also by cell-to-cell contact-dependent mechanisms. Therefore, molecules expressed on cells within the tumor, such as endothelial cells and tumor fibroblasts, as well as tumor cells, might affect axon guidance in a cell-to-cell contact manner.

It is well known that blood vessels in tumors are disorganized compared to those observed in normal tissue, and permeability is relatively suppressed in the tumor environment. Recently, a new concept has emerged whereby the normalization of blood vessels in tumors allows for penetration of anticancer drugs deep into the site of the tumors.[36] In normal tissues blood vessels are closely linked with neuronal components, suggesting that axon outgrowth accompanying angiogenesis in tumors may contribute to normalization of blood vessels in tumors. To develop new strategies for normalizing tumor blood vessels, the molecular mechanisms contributing to inhibition of axon guidance in tumors should be elucidated.

Acknowledgments

We thank K. Fukuhara for administrative assistance. This work was supported in part by a Grant-in-Aid from The Ministry of Education, Culture, Sports, Science, and Technology of Japan. There is no conflict of interest.

References

1 Willis RA. *The Spread of Tumors in the Human Body*. 3rd edn. London: Butterworths, 1973.
2 Lu SH, Zhou Y, Que HP, Liu SJ. Peptidergic innervation of human esophageal and cardiac carcinoma. *World J Gastroenterol* 2003; **9**: 399–403.
3 Levi-Montalcini R. The nerve growth factor 35 years later. *Science* 1987; **237**: 1154–62.
4 Martin P, Lewis J. Origins of the neurovascular bundle: interactions between developing nerves and blood vessels in embryonic chick skin. *Int J Dev Biol* 1989; **33**: 379–87.
5 Burnstock G, Ralevic V. New insights into the local regulation of blood flow by perivascular nerves and endothelium. *Br J Plast Surg* 1994; **47**: 527–43.
6 Mukouyama Y, Shin D, Britsch S, Taniguchi M, Anderson DJ. Sensory nerves determine the pattern of arterial differentiation and blood vessel branching in the skin. *Cell* 2002; **109**: 693–705.
7 Yamada Y, Takakura N, Yasue H, Ogawa H, Fujisawa H, Suda T. Exogenous clustered Neuropilin-1 enhances vasculogenesis and angiogenesis. *Blood* 2001; **97**: 1671–8.
8 Yamada Y, Oike Y, Ogawa H *et al*. Neuropilin-1 on hematopoietic cells as a source of vascular development. *Blood* 2003; **101**: 1801–9.
9 Takakura N, Watanabe T, Suenobu S *et al*. A role for hematopoietic stem cells in promoting angiogenesis. *Cell* 2000; **102**: 199–209.
10 Ueno M, Itoh M, Kong L, Sugihara K, Asano M, Takakura N. PSF1 is essential for early embryogenesis in mice. *Mol Cell Biol* 2005; **25**: 10 528–32.
11 Kong L, Ueno M, Itoh M, Yoshioka K, Takakura N. Identification and characterization of mouse PSF1-binding protein, SLD5. *Biochem Biophys Res Commun* 2006; **339**: 1204–7.
12 Thippeswamy T, McKay JS, Quinn J, Morris R. Either nitric oxide or nerve growth factor is required for dorsal root ganglion neurons to survive during embryonic and neonatal development. *Dev Brain Res* 2005; **154**: 153–64.
13 Toyofuku T, Yoshida J, Sugimoto T *et al*. FARP2 triggers signals for Sema3A-mediated axonal repulsion. *Nat Neurosci* 2005; **8**: 1712–19.
14 Tessier-Lavigne M, Goodman TS. The molecular biology of axon guidance. *Science* 1996; **274**: 1123–33.
15 Tanelian DL, Barry MA, Johnston SA, Le T, Smith GM. Semaphorin III can repulse and inhibit adult sensory afferents *in vivo*. *Nat Med* 1997; **3**: 1398–401.
16 Dickson BJ. Molecular mechanisms of axon guidance. *Science* 2002; **298**: 1959–64.
17 Guan KL, Rao Y. Signalling mechanisms mediating neuronal responses to guidance cues. *Nat Rev Neurosci* 2003; **4**: 941–56.
18 Semaphorin Nomenclature Committee. Unified nomenclature for the semaphorins/collapsins. *Cell* 1999; **97**: 551–5.
19 Honma Y, Araki T, Gianino S *et al*. Artemin is a vascular-derived neurotropic factor for developing sympathetic neurons. *Neuron* 2002; **35**: 267–82.
20 Kuruvilla R, Zweifel LS, Glebova NO *et al*. A neurotrophin signaling cascade coordinates sympathetic neuron development through differential control of TrkA trafficking and retrograde signaling. *Cell* 2004; **118**: 243–55.
21 Chilton JK. Molecular mechanisms of axon guidance. *Dev Biol* 2006; **292**: 13–24.
22 Eichmann A, Makinen T, Alitalo K. Neural guidance molecules regulate vascular remodeling and vessel navigation. *Genes Dev* 2005; **19**: 1013–21.
23 Chedotal A, Kerjan G, Moreau-Fauvarque C. The brain within the tumor: new roles for axon guidance molecules in cancers. *Cell Death Differ* 2005; **12**: 1044–56.
24 Bielenberg DR, Pettaway CA, Takashima S, Klagsbrun M. Neuropilins in neoplasms: expression, regulation, function *Exp Cell Res* 2006; **312**: 584–93.
25 Chedotal A, Del Rio JA, Ruiz M *et al*. Semaphorins III and IV repel hippocampal axons via two distinct receptors. *Development* 1998; **125**: 4313–23.
26 Kobayashi H, Koppel AM, Luo Y, Raper JA. A role for collapsin-1 in olfactory and cranial sensory axon guidance. *J Neurosci* 1997; **17**: 8339–52.
27 Koppel AM, Feiner L, Kobayashi H, Raper JA. A 70 amino acid region within the semaphorin domain activates specific cellular response of semaphorin family members. *Neuron* 1997; **19**: 531–7.
28 Luo Y, Raible D, Raper JA. Collapsin: a protein in brain that induces the collapse and paralysis of neuronal growth cones. *Cell* 1993; **75**: 217–27.
29 Luo Y, Shepherd I, Li J, Renzi MJ, Chang S, Raper JA. A family of molecules related to collapsin in the embryonic chick nervous system. *Neuron* 1995; **14**: 1131–40.
30 Messersmith EK, Leonardo ED, Shatz CJ, Tessier-Lavigne M, Goodman CS, Kolodkin AL. Semaphorin III can function as a selective chemorepellent to pattern sensory projections in the spinal cord. *Neuron* 1995; **14**: 949–59.
31 He Z, Tessier-Lavigne M. Neuropilin is a receptor for the axonal chemorepellent Semaphorin III. *Cell* 1997; **90**: 739–51.
32 Kolodkin AL, Levengood DV, Rowe EG, Tai YT, Giger RJ, Ginty DD. Neuropilin is a semaphorin III receptor. *Cell* 1997; **90**: 753–62.
33 Kitsukawa T, Shimizu M, Sanbo M *et al*. Neuropilin-semaphorin III/D-mediated chemorepulsive signals play a crucial role in peripheral nerve projection in mice. *Neuron* 1997; **19**: 995–1005.
34 Taniguchi M, Yuasa S, Fujisawa H *et al*. Disruption of semaphorin III/D gene causes severe abnormality in peripheral nerve projection. *Neuron* 1997; **19**: 519–30.
35 Pasterkamp RJ, Kolodkin AL. Semaphorin junction: making tracks toward neural connectivity. *Curr Opin Neurobiol* 2003; **13**: 79–89.
36 Jain RK. Normalization of tumor vasculature: an emerging concept in antiangiogenic therapy. *Science* 2005; **307**: 58–62.

Supplementary Material

The following supplementary material is available for this article:

Fig. S1. B16 tumor-conditioned medium inhibits dorsal root ganglion (DRG) axonal outgrowth, and inactivation of class 3 semaphorins rescues DRG axonal outgrowth. Immunofluorescence images of DRG primary cultures exposed to (a) control medium, (b) B16 tumor-conditioned medium, or (c) B16 tumor-conditioned medium with 50 μg/mL neuropilin-1-Fc protein. Cultured cells

doi: 10.1111/j.1349-7006.2007.00508.x

were stained with anti-β-III tubulin antibody. Shown are representative data from one of three independent experiments. Scale bar = 500 μm. (d) Statistical evaluation of the DRG halo diameter. Data show mean ± SEM from five random fields. $^*P < 0.01$.

This material is available as part of the online article from:
http://www.blackwell-synergy.com/doi/abs/10.1111/j.1349-7006.2007.00508.x
<http://www.blackwell-synergy.com/doi/abs/10.1111/j.1349-7006.2007.00508.x>
(This link will take you to the article abstract).

Please note: Blackwell Publishing are not responsible for the content or functionality of any supplementary materials supplied by the authors. Any queries (other than missing material) should be directed to the corresponding author for the article.